Instituto Tecnológico y de Estudios Superiores de Monterrey

Campus Monterrey

School of Engineering and Sciences

Development of a Novel Synthetic Coating for Abdominal Hernia Meshes

A thesis presented by

Alejandro Castañeda Sáenz

Submitted to the
School of Engineering and Sciences
in partial fulfillment of the requirements for the degree of

Master of Science

in

Nanotechnology

Monterrey, Nuevo León, June, 2020

Dedication

First of all I would like to thank God immensely, he has always been present in my life and none of this could have been achieved without him. I would like to dedicate this work to my family. A special feeling of gratitude to my loving mom and my sister. They always believe in me and gave me their unconditional confidence support and love. To my Tita who always gave me an advice and the correct words that encouraged me to pursue my dreams. I also dedicate this to my girlfriend and our beautiful baby who has supported me throughout this hard process and love. I will always appreciate all they have done.

Acknowledgements

I have very big thankful to the Research Group of Nanotechnology for Devices Design, since each one of the members gave me guidance, knowledge and friendship. I would like to thank Msc. Cintya Soria, since she was always present at every stage of this process, gave me advice, knowledge and helped me encourage and use my potential. A special thanks to Dr. Alex Elias who from the beginning always believed in me and continues to do so, in addition to giving me the great opportunity to belong to this research group and gave me his complete confidence, in addition to always challenging me to be able to demonstrate all the potential and knowledge that I have. In the same way, a thank you to Msc. Regina, Dr. Marla and Dr. Juan who always gave me their guidance, support and knowledge when I had any questions. Finally, I would like to thank David Toro, Rafael Gaxiola, Jorge Estrada, Silvia Ceceña and Jose Dominguez for their friendship and for their company in the laboratory. For those moments of laughs, stress, knowledge, and work, without you this would have been twice as difficult. The author of this thesis would like to thank financial support from Tecnológico de Monterrey through the Research Group of Nanotechnology for Devices Design, and from the Consejo Nacional de Ciencia y Tecnología de México (Conacyt), Project Numbers 242269, 255837, 296176, National Lab in Additive Manufacturing, 3D Digitizing and Computed Tomography (MADiT) LN299129 and FODECYT-296176.

Development of a Novel Synthetic Coating for Abdominal Hernia Meshes

by

Alejandro Castañeda Sáenz

Abstract

Through the years hernia problems have become more common around the world. The use of medical devices (hernia mesh) in surgical procedures help to reinforce soft tissue's defects and give support to the human body. However, these devices are related with post-operative drawbacks as inflammation, adhesion, infection, incorporation, and many others, being the last one the most challenging to solve. Due to this, coating materials have been used in order to reduce complications and improve incorporation with the organism. This master thesis project focuses on the development of synthetic coating material for hernia mesh capable of decreasing post-operative complications and improving incorporation and adaptability, also promoting tissue regeneration for 500,000 patients suffering from this pathology in Mexico. To achieve this goal, composite polycaprolactone (PCL) membranes were prepared using different biomaterials as hyaluronic acid (HA), vitamin E, xanthan gum (XG), polylysine, and others at different concentrations by solvent casting method in N,N- Dimethylformamide (DMF) and chloroform (CL). Surface morphology revealed changes in the porosity and in the mean pore size produced by the solvent-polymer interactions, as well as by the inclusion of biomaterials, obtaining specific pores allowing cell migration and proliferation. The changes in crystallinity and melting temperatures were measured by X-ray Diffraction (XRD) and Differential Scanning Calorimetry (DSC), showing lower crystalline values in composite membranes due to the addition of amorphous materials and solvent interactions, creating lower density hydrogen bonds and disrupts in the polymer chain. Different ratios in evaporation of solvents could affect structural changes in the material. Also, the presence of crystalline planes (110), (111), and (200) could be observed indicating an orthorhombic unit cell corresponding to PCL nature. Functional groups were found by FT-IR analysis, showing vibrational bands at 3350 cm1 (-OH and -NH groups), 2837 cm1 and 2867 cm1 corresponding to an asymmetric and symmetric stretching modes (C-H hydroxyl (CH=O)) confirming the presence of polymer and biocomponent. Furthermore, there was no creation or elimination of new bands, therefore it is inferred that there is a good affinity and interaction of solvents. Contact Angle (CA) technique showed both hydrophilicity and hydrophobicity behavior. However, most of the samples showed angles between 70^{o} and 90^{o} referring hydrophilicity which is beneful for stem cell attachment and cell migration. Finally, non-Newtonian and hyper-elastic behavior could be observed in rheology properties due to changes in polymer chain giving stiffness and re-orientation of molecules. Therefore, it was possible to develop a prototype of an intelligent synthetic coating for abdominal wall hernia meshes with superior characteristics to the commercial ones, and with significant advances in the state of the art, which will give the possibility of preserving abdominal wall integrity to patients suffering from this problem.

List of Figures

List of Tables

Contents

Chapter 1

Introduction

We can define a hernia as an organ that projects itself through the extracellular matrix or the cavitity that contains it breaking that wall (figure 1.1)[1]. The surgical repair of abdominal wall hernia consists in re-positioning the organs into the abdominal cavity, to then can close and reinforce of the defect using either a suture or a net-like prosthesis (called mesh).

The use of surgical mesh for hernia repair has become widespread in recent years. At least 500,000 people in Mexico and 20,000,000 people in the world are affected by hernia issues causing pains, wounds, and in worst cases death. In other countries as the United States 750,000 surgical procedures are developed each year and growing [2].

One of the most common types of hernias are inguinal with 75% of all abdominal hernias. According to literature males and females are propense to this and at least 27% of mens and 3% of womens have this problematic [3]. Considering all groin hernias can be stipulated that 96% of them are inguinal, while the 4% are femoral. Also, men are more likely to have a hernia, while women are 20 times more likely to need a repair [4].

The first approach to solve this problematic was the creation of a mesh capable to reinforce, support and close the wound generated by a hernia. In the 1950s the first mesh made of polypropylene was approved and implanted [5]. Afterwards other materials came like polyester, polyurethane and polytetrafluoroethylene providing different properties and characteristics. Nevertheless, one big disadvantage associated with surgical meshes is the drawbacks generated by these. Inflammation, infection, shrinkage, adhesion, and many others are some examples.

An important point to consider is that these drawbacks come after the ambulatory process. Therefore, the post-operative stage is very important. According to Jenkins in 2008,

the average time for recovery from a hernia surgical process is seven to fourteen days, so it is vital to avoid these complications [3], specially the inflammatory response due this stage could produce fibrosis and other problematics.

Due to this, different types of biocompatible materials have been investigated and analyzed for its use in surgical meshes and to improve their properties. Currently, the use of alginate and chitosan for the generation of drug-carrying particles has been postulated as an option for the treatment of the infectious and inflammatory response. However, there still other complications that these biomaterials cannot solve and for that the development of coatings was made.

The coatings are materials that covers surfaces and cause modifications to improve and/or protect the properties of the material [6], due this, its use in biomedicine has grown the last years. Actually, biomaterials as hyaluronic acid, vitamin E, collagen, polyethylene glycol and many more have been used to the development of hydrophilic and hydrophobic coatings for surgical meshes, providing improvements in drawbacks related to adhesion, proliferation and biocompatibility, moreover, the use of stem cells added to a coating have helped in the repair of the abdominal wall [7].

Stem cells today represents an alternative to problems in regenerative medicine. These cells are capable of self-regeneration and producing new cells capable of transforming into multiple cell types [8]. With this, problems such as tissue, organ, congenital defect and disease repair can be attacked, which is why regenerative medicine has great relevance in the use of stem cells [9].

The addition of PCL with these kinds of biomaterials has been poorly investigated, but it has shown that improves healing effects. For this and to further advantages of this composite material, this paper is focused on the preparation and the physicalchemical and biological properties of novel PCL membrane elaborated by using chloroform and N,N - dimethylformamide (DMF) solvents, also, with the inclusion of hyaluronic acid, vitamin E to finally implant and growth stem cells. To perform the experimental stage, a DoE was developed, and all the samples were studied by different techniques. The morphological changes produced by the solvents and the organic material will be performed by Scanning Electron Microscopy (SEM). The surface permeability and roughness conditions will be explored by Contact Angle (CA) respectively. Structural properties will be measured by X-Ray Diffraction (XRD) and by Differential Scanning Calorimetry (DSC) to detect changes in the polymeric crystal

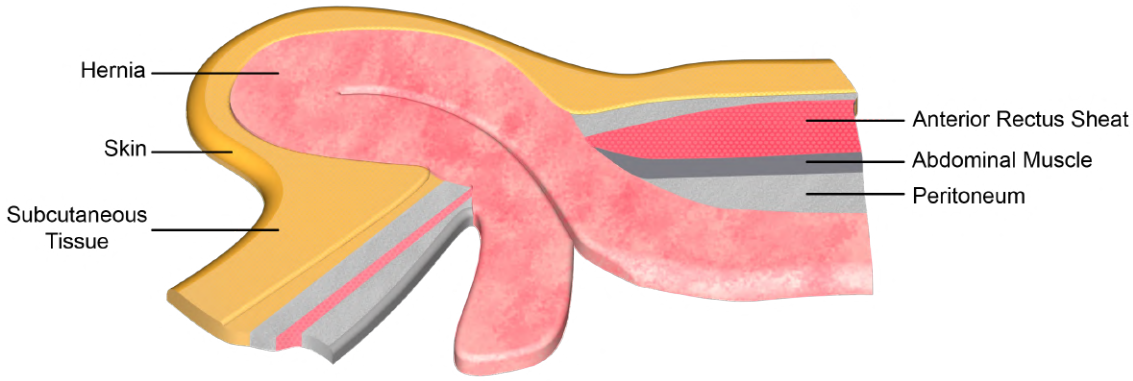

Figure 1.1: Representative illustration of a protrusion of an organ, where it can be seeing the abdominal muscle, subcutaneous tissue, the peritoneum and the skin.

domain. While, all the chemical interactions will be studied by Fourier-transform infrared spectroscopy (FTIR) analyses. To evaluate the rheological behavior (viscoelastic properties) a rotational rheometer was used.

1.1 Problem Statement and Context

Nowadays, the use of surgical meshes has grown because at least 500,000 people in Mexico and 20,000,000 people in the world are affected by hernia issues causing pain, wounds, ambulatory processes resulting in more than 4 million dollars in associated expenses (in Mexico). In general, surgical meshes have different drawbacks associated with, including infection, inflammation, adhesion, etc., furthermore, mesh incorporation is one of the biggest challenges to solve due to the human body does not recognize the mesh as own causing a big foreign body response which comes along with pain, discomfort and in some cases death to the patient.

1.2 General Objective

Develop a synthetic functional, biocompatible and bioabsorbable coating for an abdominal wall hernia mesh with hyaluronic acid, vitamin E and adipose tissue stem cells, which will help to reduce post-operative problems such as tissue incorporation, inflammation, in addition to improving adaptability and cell proliferation.

1.2.1 Specific Objectives

1. Synthesize a coating for an abdominal wall hernia mesh composed by polycaprolactone, hyaluronic acid and vitamin E.

2. Do the physical, chemical and biological characterization of the coating.

3. Design a prototype of a coating for an abdominal wall hernia mesh.

1.3 Justification

Commercial surgical meshes present post-operative complications, such as infection, inflammation, adhesion and poor incorporation with human body, which is why it is necessary to develop a cover that helps to solve this problem.

1.4 Hypothesis

The modification of surface mesh with hyaluronic acid, vitamin E and stem cells can improve integration with the body by promoting growth factors, ECM components and cell proliferation reducing low foreign body reaction and hence post-operative drawbacks.

Chapter 2

Hernia mesh: principles, materials and properties

2.1 Stages of surgical meshes

2.1.1 First generation

Since the introduction of polypropylene in the 1950s, it has been the predominate material used for hernia repair thanked to its great properties and biocompatibility. An important characteristic is that these are heavyweight (>140 g/m2), engineered to withstand pressures greater than 100 N/cm, unfortunately this led to a sensation of stiffness and a perception of the mesh in the abdominal wall.

These meshes are classified into three categories: macroporous meshes (75 um), microporous meshes (10 um) and macroporous meshes (75 um) with multifilament components [1].

Most meshes made of polypropylene have the characteristics of being inert to the human body and not being absorbable, hovering in a pore size between 0.02 mm - 2.5 mm. According to Kalaba in 2016, it describes that synthetic materials are mostly used in hernia repair surgeries, such as polypropylene or polyester, these can generate certain histopathological processes and unwanted immunological reactions[10]. Different types of hernia meshes can be observed in table 2.1.

Brown Finch in 2010, worked with Polyglactin using a small pore size (0.4 mm), a medium weight (56 g/m2) and polyglicolic with a medium pore size (0.75 mm), both materials degraded completely between 60 and 90 days. In this investigation he found that these

two materials possess properties that decrease the risk of infections. Although, being absorbable by the body, usually end in recurrence of hernia [5]. In addition, Zhang et al. in 2016 conducted several investigations about generic meshes made of different materials such as Polyvinyl alcohol (PVA) modified PP mesh (PP / PVA), poly (vinylalcohol), performing in vivo tests on rabbits modifying some antibacterial or non-stick characteristics, favoring biocompatibility with the body, but no significant changes were observed regarding the inflammation generated by this mesh [11].

2.1.2 Second generation

In this, researchers had focused on the previous drawbacks caused by polypropylene and other materials. These drawbacks include recurrence, adhesion risk, infections, etc. besides this the based material was still polypropylene. The most remarkable difference is that this generation is a combination of materials like collagen, omega-3, titanium, polylactic acid, and many others as Baylon et al., points out. The main advantage of these composite meshes is their use in intraperitoneal spaces due it causes minimal adhesion formation.

An important characteristic is that these meshes requires a specific orientation due the visceral side has the “adhesion barrier”, a microporous surface that will help to prevent this issue.

These types of meshes have great advantages compared to the synthetic ones because in addition to having the mechanical properties of the material of a synthetic material the coating provides more specific characteristics and favors the correction of possible complications such as visceral adhesion, high tissue integration and decrease the risks of infection. With ranges of pore size between 0.84 mm to 3.5 mm, mostly with monofilament, these are partially absorbable or non-absorbable. Different authors (table 2.2) evaluated composite meshes having excellent results in adhesion, recurrence and infection drawbacks.

2.1.3 Third generation

This generation was focused on a new kind of materials, a new proposal for new properties and better biocompatibility. The second generation left the prevalence of adhesions and it was necessary the use of new material. Biologic materials were the main base on these meshes as human dermis, bovine and porcine pericardium as can be see in table 2.3. These were derived

Table 2.1: First generation of hernia meshes made of synthetic materials

Product Author	Manufacturer	Material	Advantage	Disadvantage	Absorbable	Pore Size	Filament
Vycril [1] [12] [13]	Ethicon	Polyglactin	Infectious disease risk is eliminated	Usually results in hernia recurrence	Yes, fully (60–90 days)	0.4	Multifilament
Dexon [5] [14]	Covidien	Polyglycolic	-	Usually results in hernia recurrence after	Yes, fully (60–90 days)	0.75 mm	Multifilament
Marlex [15] [16] [17]	Bard	Polypropylene	Inert, used in most woven prostheses	Rigid	Non absorbable	Between 0.2 - 0.7mm	Monofilament
Safil [18] [19]	Braun	Polyglycolic	Low risk of late secondary infections	Rapid mesh degradation and high reccurrence rates	Yes, fully (60–90 days)	0.25mm	Multifilament
Prolene [15] [20] [21]	Ethicon	Polypropylene	Inert, used in most woven protheses	Rigid	Non absorbable	1 - 1.6mm	Double filament
Surgipro [10] [22] [23]	Covidien	Polypropylene	Excellent visibility, Retains properties in-vivo	-	Non absorbable	0.8mm	Mono + multi filament
Parietene [15] [24] [25]	Covidien	Polypropylene	Inert, used in most woven prostheses	Rigid	Non absorbable	1.5mm	Monofilament
Fluoropassiv [26] [27] [28]	Vascutec	Polyester with fluoropolymer and gelatin	More hydrophilic, better biocompatibility	-	Partially	Macrophorus	Multifilament
Gore-Tex [1] [29] [30] [31] [32]	Gore	ePTFE	Decrease mesh complications	Very high reherniation-rate	Non absorbable	0.003mm	Multifilament
Serapren [1] [20] [33]	Serag-Wiessner	Polypropylene	-	Inflammation and fibrosis	Non absorbable	0.08 - 0.1mm	Mono + multi filament
Prolite [33] [34]	Atrium	Polypropylene	Optimal burst and fixation retention strength	inflammation, fibrosis and permanent elongation	Non absorbable	0.6 - 0.8mm	Monofilament
Optilene [33] [35]	Braun	Polypropylene	Reduce chronic pain	Inflammation and fibrosis,	Non absorbable	1 - 3.6mm	Monofilament
Atrium [1] [36]	Atrium	Polypropylene	High tolerance to infection	Adhesion risk	Non absorbable	0.8mm	Monofilament
BardSoft [10]	Bard	Polypropylene	60% lighter than traditional polypropylene mesh	-	Non absorbable	2.5mm	Monofilament
Mersilene [10] [36]	Ethicon	Polyester and PET	Low rate of complications and recurrence	Incidence of infection	Non absorbable	1mm	Multifilament
DualMesh [16] [10] [37]	Gore	ePTFE	Good incorporation of tissue and weaker FBR	Risk of serious bowel injury	Non absorbable	0.003mm	Foil
MycroMesh [10] [38] [39]	Gore	PTFE	Good vascularization	-	Non absorbable	0.025 - 0.3mm	2mm perforations
Mosquito net mesh [40]	Generic mesh	Polyester with PET	No citotoxicity and good cell proliferation	High recurrence rate and infection	Non absorbable	2 x 2.3mm	Multifilament
Experimental mesh [11]	Generic mesh	PP with PVA	Anti-adhesion efficacy	-	Partially	-	-
Experimental mesh [41]	Generic mesh	PP with b-cyclodextrins	Antibacterial effect	-	Non absorbable	3.5 x 2.5mm	Monofilament
Experimental mesh [42]	Generic mesh	PP with chitosan and PLGA	Anti-adhesion efficacy and tissue integration	Weaker antimicrobial efficiency	Non absorbable	-	Monofilament
Experimental mesh [43]	Generic mesh	PVA	Good tissue integration and low adhesion	-	Yes	Small pore	-
Experimental mesh [44]	Generic mesh	Poly(succinimide)	Hydrophobic and biocompatibility	Are not used in hernia repair yet	-	-	-
Experimental mesh [45]	Generic mesh	Cyclodextrin onto polyester	Prevention of infection	Not evaluated in vivo	Non absorbable	-	Multifilament

Table 2.2: Second generation of hernia meshes based on composite materials

Product Author	Manufacturer	Material	Advantage	Disadvantage	Absorbable	Pore Size	Filament
Proceed [46] [47] [48] [49]	Ethicon	PP surrounded by PDS coated with cellulose	Feasible and has a low complication rate	Shrinkage	Partially absorbable	3.5 x 2.5 mm	Monofilament
Sepramesh [50] [29] [51] [52] [53]	Bard	PP mesh with sodium hyaluronate/CMC	Prevent adherence and great mesh incorporation	Promotes the separation of healing tissues	Partially absorbable	Macroporous	Monofilament
Ultrapro [5] [10] [29] [54]	Ethicon	PP and PGA with PCL	Decrease risk of infection	Adhesion issues	Partially absorbable 90 - 120 days	2 - 4mm	Monofilament
Dynamesh [46] [55] [56] [57]	FEG Textiltechnik mbH	PP with PVDF	They do not curl up and retain its shape	Not induce adhesion to visceral organs	Non absorbable	1mm	Monofilament
Ti-Mesh [46] [51] [58] [59] [60] [61]	PFM Medical	Polypropylene with Ti coat	Low shrinkage rate	Mild chronic inflammatory reaction	Non absorbable	$>$1mm	Monofilament
Vypro and Vypro II [62] [63] [64] [16]	Ethicon GmbH	Polypropylene with polyglactin 910	Better compliance and less chronic pain	Higher rate of hernia recurrence	Partially (8 weeks)	1 - 2.5mm	Multifilament
Parietex [65] [55] [66] [67]	Covidien	Poliester and collagen	Short term benefit for anti-adhesion property	-	Partially (20 days)	1.8 x 1.5mm	Monofilament
Symbotex [68] [69] [70]	Medtronic	Polyester coated with collagen film	Minimizes tissue attachment to the mesh	-	Partially	2.1 x 3mm	Monofilament
Prevadh [71]	Covidien	Oxidized bovine type 1 with PEG and glycerol	Anti-adhesion property and effective in decreasing inflammation	Needs rehydration	3 weeks	-	-
Surgiwrap [10] [71]	Mast Biosurgery	PP 70:30 PLA	Excellent tissue integration	Adhesion formation	6 - 8 weeks	Macroporous	Monofilament
Ventralight ST [72] [73] [74] [75] [76]	Bard	PP and PGA	Minimize adhesion formation between the mesh and the viscera	-	PP non absorbable, PGA absorbable	$0.84 \pm 0.04mm$	Monofilament

Table 2.3: Third generation of hernia meshes based on biological grafts

Product Author	Manufacturer	Source	Advantage	Disadvantage	Absorbable	Pore Size	Cross-linked
AlloMax [77] [78] [79]	Bard/Davol	Human dermis	No mesh infection	Rehydration needed	2 -3 months of degradation	-	-
AlloDerm [78] [80] [81] [82]	LifeCell	Human dermis	Can be used in contaminated wounds	Rehydration and tends to stretch	2 -3 months of degradation	-	No
Veritas [83] [84]	Synovis	Bovine pericardium	-	-	2 -3 months of degradation	-	No
SurgiMend [78] [83] [84]	TEI Biosciences	Fetal bovine dermis	Low hernia and bulge recurrence	Rehydration needed	2 -3 months of degradation	-	No
Permacol [78] [85] [84]	Covidien	Porcine dermis	At large sizes no refrigeration or rehydration needed	-	2 -3 months of degradation	-	Yes
Strattice [85] [84]	LifeCell	Porcine dermis	No rehydration and large sheets	Decrease in tensile strength	2 -3 months of degradation	-	No
XenMatrix [86] [87] [88]	Bard	Porcine dermis	Range of sizes and excellent tissue integration	-	2 -3 months of degradation	-	No
Flex HD [89] [90] [91] [92]	MTF/Ethicon	Human dermis	Great tensile strength and tissue integration	Unable to additional sterilization	2 -3 months of degradation	-	No
Surgisis [59] [19] [93] [94]	Cook	Human xenograft	Low foreign body reaction	Decrease in mechanical strength	2 -3 months of degradation	-	-
Experimental mesh [95]	Generic mesh	carbodiimide cross-linked cholecyst	Optimal tissue response and degradation rate	-	Aprox. 56 days	-	Crosslinked
Experimental mesh [96]	Generic mesh	Bacterial nanocellulose	Good fixation in tissue	-	Yes, 60 days	-	-
Tutopatch [65]	RTI surgical	Bovine pericardium	Low inflammatory response	Lack of information	Yes	-	-
Fortagen [10] [65]	Organogenesis	Xenogenic	No hydration	Crosslinking may disrupt tissue integration	Yes	-	Crosslinked
Dermal Matrix [97]	-	Porcine dermal matrix	Lower infection rates and hernia recurrence	-	Yes	-	-

from donors of decellularized sources. A big feature on these meshes is that these materials do not have an inflammatory reaction on the body. An inconvenient with this generation is that the cost is highly elevated compared with previous generation, also an important point has to be considered and is that they need hydration every so often.

This type of surgical meshes is one of the best options in terms of mechanical performance, also they come from human skin tissues, porcine and bovine sources, because of this there exist a great biocompatibility.

The meshes made from sections of human skin are very useful since these can be used in contaminated wounds or placed without generating any infection and being absorbable. However, it is necessary to rehydrate them due to previous treatments that are affected. These meshes take about 2 to 3 months to degrade. In addition, xenographic human tissues can be used favoring the reduction of the formation of a mesoma, in a short period of time it loses its mechanical strength. Added to this, porcine meshes have a wide range of sizes and do not require rehydration which makes the practices easier to use. However, according to Huntington, who compared 5 different non-crosslinked meshes of this type, he found that they have a high rate of infection, inflammation, allergy, adhesion or fistula formation [79].

As for the bovine skin base, a low inflammatory response has been found, and in some cases the recurrence in the hernia because it degrades approximately between 2 and 3 months. There is little information about this type of mesh.

2.1.4 Fourth generation

Besides the effort to eliminate or reduce drawbacks on meshes of previous generations, these were still affecting, specially recurrence. The hybrid mesh as there are called have the main difference that are develop with the form of a “sandwich”. It has a first base made of biological grafts, then a layer of synthetic material is placed (polypropylene is the most popular material) and finally there is another layer of biological graft to close the mesh. In this model the biological grafts are estimated to be absorbed by the body leaving the layer of the synthetic material as the “wall” in the body. Actually, the market for these meshes are very restricted. Cook Biotech is a company that is developing surgical meshes with this features. Their first mesh called Zenapro^{TM} is made of polypropylene within a matrix of small intestinal submucosa (SIS) and has large pores to bring strength to the mesh [98]. Hodde and coworkers evaluated a Zenapro mesh for histological and adhesiogenic behavior. In their main outcomes

Zenapro decreases adhesion issues provoked by the nature of polypropylene due proteins and components provided by SIS to the extracellular matrix, also maintain tensile strenght and tissue ingrowth. Other authors have tested another kind of hybrid mesh like Ovitex resorbable and Ovitex permanent mesh against Zenapro mesh, Syneroc Phasix mesh, finding that hybrid mesh Syneroc showed lower abscess scores than the others, also, Zenapro and Ovitex (both models) showed significant bacterial colonization, which may be occur by the mat-like mesh structure [99]. However, further studies are needed to completely evaluate this hybrid meshes.

2.2 Coatings

Due to the complications presented in conventional meshes such as inflammation, infection, adhesion and biocompatibility, an investigation has been generated for the development of mesh coatings and in this way to solve these problems. According to research when coating these meshes with biomaterials and / or antimicrobial agents helps to increase tissue growth [55], in addition a fundamental part is the thickness of the coating, however there is no perfect thickness and it can vary from the nano to the microscale [100].

Since polypropylene mesh is the most common, it has been characterized as being the most studied to modify its surface with different materials.

These coatings are produced from synthetic (absorbable and non-absorbable) and biological materials, an scheme can be seen in figure 2.1 Absorbable materials are used mostly because the mesh is sought to have a temporary protection to avoid the risk of adhesion formation. Some of these materials are: polylactin, polyglecaprone, titanium, gelatin, carboxymethyl cellulose, zein, alginate, fibroblasts, stem cells, hyaluronic acid, omega-3, etc

Different authors (table 2.4) have evaluated the actions that these coatings have on mesh for a hernia. Yelimlies [101], Kyzer [102] and Van 't Riet [103], agree that, coatings made of carboxymethyl cellulose (CMC) and collagen help reduce the risk of adhesions in polypropylene meshes due CMC works as a barrier with visceras , on the other hand as reported by Klinge [104], Lehle [105], Scheidbach [106] and Junge [75], gelatin, fluorocarbon and titanium nitride are excellent for promoting the growth of native tissue during wound healing coupled with no a risk of toxicity to the patient. Zhao [107], coated a polypropylene mesh with adipose tissue stem cells to reduce the inflammatory response. Similarly Zhu [34], mentions that polypropylene meshes with titanium have been shown to reduce the inflammatory reaction of the body. Other materials such as chitosan, liposomes, folic acid, polyethyleneamine

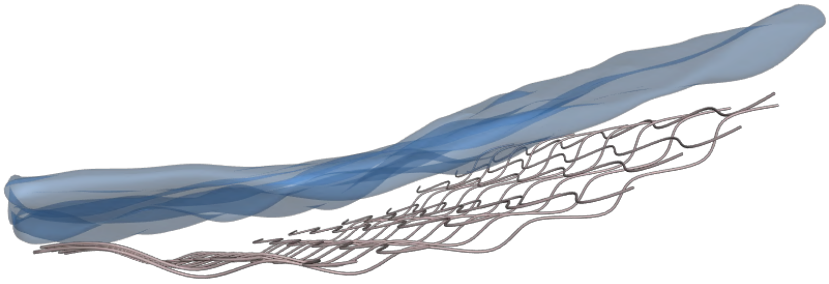

Figure 2.1: Design of a coating for a surgical mesh.

and vitamin E may be beneficial to improve the biocompatibility of meshes.

The use of biomaterials as coatings for hernia meshes has proven to be of great benefit by helping to solve or reduce these drawbacks. These meshes are considered as composite meshes due to the physical and chemical conformation they possess. Despite this, post-operative problems are not fully solved and further studies are necessary to find new materials and new solutions to these complications.

2.3 Properties

2.3.1 Pore Size

Pore size represents a fundamental part of surgical meshes, depending on pore size, both, benefits and post-operative complications can be generated. If the pore size is very large, can help to the proliferation and cell infiltration of macrophages and fibroblasts, however, this can lead to complications since it serves as the cradle of bacteria that can affect the patient, in addition to being seen to generate adhesion. If the pore is too small it can help to prevent fibrosis through the mesh, but it can prevent tissue growth and cell movement due to size, in addition to generating small adhesion [5], [46], [10].

The pores can be classified by types/groups where the size varies between 0 and 2000 um:

1. Large pore $>$ 2000 um
2. Long pore 1000 - 2000 um
3. Normal pore 600 - 1000 um

Table 2.4: Synthetic, biological and inorganic materials for the development of coatings

Coating	Mesh material	Action	Advantage	Disadvantage	Author
Polyglactin	Polypropylene	Increase hot tissue ingrowth	Non antigenic, minimal tissue reaction	Some tissue drag	[104] [108]
PEG	Polypropylene, Polyester	Fibroblast grow faster and in greater number	Can work as a vehicle for drugs	Tend to be more irritating	[109] [110] [111]
PVA	Polypropylene	Anti adhesion barrier	Non toxic	May increase inflammation formation	[11]
Gelantin and Fluorocarbon	Polyester	Increase biocompatibility	Can be used as a drug carrier	-	[26] [112]
Gold	Polypropylene	Prevents bacterial colonization	Inert, non toxic and biocompatibility	Low body clearance	[113] [114]
Titanium carbonitride	PP, PTFE	Increase host tissue ingrowth	-	-	[106] [75]
Gold-Palladium	Polypropylene	Prevents bacterial colonization	Inhibit adhesion of bacteria and biocompatibility	Low toxicity	[113]
Human fibroblast	PP, PGA	Wound healing and inflammation response	Regulation of inflammation and wounds	Postoperative discomfort	[115] [116]
Silver	PET	Reduces bacterial attachment	Good against bacteria	Less capacity to load drugs	[117] [118]
Platinum	-	Coating for nanoparticles	Low corrosivity and biocompatibility	-	text
Silica Oxide	Polypropylene	Antibacterial effect and afford cell growth	Anti adhesion effect	-	[119]
CMC	Polypropylene	Significantly reduces adhesion	Reduce adhesion	-	[101]
Collagen	Polypropylene	Decrease adhesion rates	Facility, viability and attachment	Increase infection rates	[103] [102]
Vitamin E	Polypropylene	Anti inflammatory effect	Anti inflammatory effect	Highest doses are harmful	[120] [121] [122]
ePTFE	Polypropylene	Reduce adhesion effect	Great mechanical properties and chemically inert	Can produce fibrosis and shrinkage	[123] [124] [125]
Omega 3	Polypropylene	Enhance fixation and handling	Minimal inflammatory response	-	[66]
Chitosan	Polypropylene	Decrease fibrosis	Reduce inflammaroty response and reduces fibrosis	-	[126]
Trimethylene carbonate	PTFE and PGA	Low recurrence rates	-	-	[127] [128]
Hyaluronic acid	Poly-4-hydroxybutyrate	Reduction of bacteria contamination	Promotes proliferation and infiltration	-	[127]
Rifampicin	Bovine dermis	Promotes antibacterial effect	Antibiotic	-	[127] [129]
Poliglecaprone	Polypropylene	Help avoiding adhesion of PP	Mild tissue reaction and high tensile strength	Rapidly decrease of tensile strength	[127] [130]
Titanium	Polypropylene	Reduce inflammatory reaction	Biologically inter and good biocompatibility	Poor tribological performance	[34]
Mesenchymal stem cell	Polypropylene	Reduce inflammatory reaction	Reduce tissue adhesion and inflammatory response	Differentiation process	[107]

4. Small pore 100 - 600 um

5. Micro pore $<$ 100 um

Some synthetic and biological meshes such as: Prolene, Fluoropassiv, Optilene, Bard-Soft, Ultrapro and Sepramesh have a large pore size (1 - 4 mm), while Serapen, Vycril, Marlex, Surgipro, Goretex handle a small pore size (0.003 - 1 mm) (table 2.5).

Judge et al. [50], analyzed two commercial meshes, Parietex composite mesh (PCM) and Sepramesh (SM), where they found that the PCM mesh had a larger pore size, also infer that this can help to improve the incorporation process as it improves tissue growth. Klinge [104], mentioned that small pores (between 100 - 200 um) inhibit fluid transport, which prevents tissue growth, however in a small pore polypropylene mesh they found an increase in the foreign body response. Chu and Welch [131] mentions an analysis to observe how the adhesion of tissue with different pore sizes (5 - 20 um, 20 - 50 um, 50 - 200 um) behaves, in which they performed mechanical tests in order to find the optimal pore size, finding that the size of 50 - 200 um is the best.

2.3.2 Weight

It is well known that meshes for hernia generate post-operative complications due to the characteristics/properties they possess. An example of this is polypropylene mesh which has problems such as chronic inflammation, chronic pain, foreign body reaction, etc. Due to this, so-called low density meshes have been developed, which are characterized by causing a reduction in the volume of polypropylene and increasing the pore size [132]. These meshes have an approximate weight of 33 g/m^2. On the other hand, there is another type of category, high density meshes (100 g/m^2), which are characterized by small pore sizes and high tensile strength, in addition to generating foreign body reaction [5]. Bilsel [65], mentions that there is no significant difference between high and low density meshes in terms of tissue incorporation, tensile strength or inflammatory response.

Due to all this a system was proposed to identify the meshes based on their weight, so it was divided into 4 categories [133]:

1. Ultra-light $<$ 35 g/m2

2. Light $\geq$ 35 $<$ 70 g/m^2

3. Standard $\geq$ 70 $<$ 140 g/m^2

4. Heavy-weigth $\geq$ 140 g/m^2

In the same way Coda [133], mentions another classification made in 2008 by other authors [134], in which they handle similar values. Ultra-light $<$ 35 g/m^2, light 35 - 50 g/m^2, standard 50 - 90 g/m^2 and heavy-weight $>$ 90 g/m^2

2.3.3 Bio-mechanical properties

These properties refers to the necessary values of an abdominal wall mesh to support and avoid possible post-operative drawbacks, in other words, has to mimic natural tissue (see table 2.5). By guaranteeing the minimum force necessary to resist abdominal forces (16 N/cm), the risk of mechanical overloads during implantation and the lifetime of the material would be eliminated. In the same way, a minimum abdominal pressure of 1 – 6.5 mmHg should be guaranteed in older adults and high stiffness values are related to tissue erosion and other kind of complications. By controlling the degradation time of the polymer, could be achieve a balance and control between degradation and regeneration capacity of the material, since it has been demonstrated in the literature that by achieving this, there can be improved flexibility, cellular inflation, and mechanical properties. Stem cells plays an important role here due to they would be responsible for this control by segregating components of the extracellular matrix [135, 136].

Elasticity

According to the literature, the natural elasticity of the abdominal wall is at 32 N/cm (38%) [5]. Knowing the elasticity allows us to predict more efficiently how the mesh will behave once it is implanted. A surgical mesh with low elasticity is prone to restrict the movement of the abdominal wall causing pain and complications. It is recommended that the minimum elasticity be 16 N/cm [15].

DuBay et al. [137], mentioned that elasticity is one of the most significant factors for the prevention of recurrence of hernias. Not having the minimum elasticity can result in complications during and after mesh implantation. Therefore, the selection of heavy meshes for hernia repair will result in the restriction of the expansion of the human abdominal wall. On the contrary, if the material of the light meshes has a greater elasticity than the human abdominal wall, their function will be deficient and there will be a recurrence [41].

Sanbhal [41] state that the elasticity of the mesh in ranges from 15% to 30% at 16 N/cm, provides favorable behavior in human body, because the device can achieve a maximum of

38% at 32 N/cm. However, Kalaba et al. [10], found that even extending the range from 11% to 32% the same results remain. Some of the meshes that meet these requirements are Marsilene, AlloMax, FlexHD.

Tensile Strength

Tensile strength represents a very important parameter to consider for the behavior of the mesh since after implantation if there is a weakening in this property, the mesh can cause a structural failure, causing an extirpation. The weight of the mesh has to be taken into account to avoid decrease strength values due to weight reduction [34].

According to an experiment conducted by Barreiro et al. [138], the maximum tensile strength that supports the abdominal dermis is 403.5 $\pm$ 27.4 N. However, in another analysis performed by Deeken and Lake [139], they assume an extreme case, where the intra-abdominal pressure rises. With this, the tensile stress will have a value of 47.8 N/cm, so it is recommended that the hernia repair materials be at least 50 N/cm (table 2.5).

Other studies have shown that at the value of 16 N / cm of tensile force, both men and women have a natural distension in the horizontal and vertical direction, where the values are around 23 7% for men and 32 17% for women [1], [140].

Stiffness

Stiffness represents and has a great influence on the performance or surgical meshes. If they are too rigid they are prone to open the abdominal wall tissue and cause pain to the patient at the time of making a movement [137]. On the other hand, if the mesh is very soft it will not be strong enough. This property is taken into account when manufacturing a mesh, no values have been standardized for it [15].

The companies in the market have varied the values in each of the different meshes with a range between 0.9 N/mm which have enough flexibility such as Parietene® and Optilene®. Most biological meshes coincide with the same stiffness values that are around 58.3 N/mm according to Kalaba [10]. However, the most predominant values synthetic meshes are 0.9 to 4.6 N/mm. It is necessary to pronounce that stiffness and other bio-mechanical properties could change after the mesh implantation.

In the same way, the material composition dictates also the properties that the mesh may

Table 2.5: Recommended biomechanical values to guaranty optimal behavior and safety of the mesh [5, 34, 135]

Properties	Recommended Values
Tensile Strength	Minimum: 16 N/cm Normal: 32 N/cm
Stiffness	0.9 - 5 N/mm
Abdominal Pressure	Normal pressure: 1 – 6.5 mmHg When jumping of coughing: 170 mmHg
Elongation	20% / 40%
Orientation	To assess similar physiological stretchability specific orientation is needed (select right side)

have. Polypropylene is a material that has excellent mechanical properties as tensile strength, stiffness, mechanical stress and flexibility, however, the manufacturing process changes these properties due the anisotropic or isotropic behavior but in most of cases improves these properties. PTFE is a microporous material with good strength and stiffness and posses good low adhesive and inflammatory values, in comparison with polyester that has shown higher adhesion values and lower stiffness and it is not recommended to be implanted in the peritonium area unless it has an anti-adhesive layer [141].

2.4 Porogens

A very important aspect to mention is that porous can be manipulated to improve the properties of a mesh or of a coating, i.e., with specific pores. This effect is called porogen. A porogen part of diluents (solvents), which are used to dissolve polymers this allows to create modifications to the surface of the material, the type, pore size, the morphology among other factors. To create pores, porogens called solvating and non-solvating are used. This characteristic is defined by the polarity, the crosslinker and the solubility parameter of the polymer, also this help to classify as good or bad diluents, in other words, it has a good or bad miscibility. Generally, the solvating porogen provides to the polymer a large surface area and creates micropores, while the non-solvating porogens provides a small surface area but develops large pore size as it can be seen in figure 2.2. This is because the property of a pore-generating solvent affects phase separation that influences in the properties of the polymer. Another important fact is that the size of the surface can be modified by varying the concentration of the crosslinker to be used [147, 148].

Table 2.6: Physical and mechanical properties of different surgical meshes available in the market

Mesh	Weight	Pore size	Mesh category	Tensile strength/Tensile stress	Stiffness	Burst strength	Elasticity	Shrinkage	Author
Vicryl	56 g/m^2	0.4 mm	Lightweight	78.2 $\pm$ 10.5 N/cm	4.6 $\pm$ 0.5 N/mm	-	-	-	[25], [1], [5]
Marlex	95 g/m^2	0.2 - 0.7 mm	Standard	2.59 MPa	57.2 N/cm	4.5 $\pm$ 0.12 kg/cm^2	13.7	-	[65], [5], [10], [131], [142]
Prolene	105 - 108 g/m^2	1 - 1.6 mm	Standard	2.46 MPa	3.6 $\pm$ 0.4 N/cm	156.6 $\pm$ 9.2 N/cm	6.9 N	-	[25], [65], [10], [142], [143]
Surgipro	110 g/m^2	0.8 mm	Standard	3.25 MPa	1.3 $\pm$ 0.3 N/mm	-	-	10.42 $\pm$ 3.52%	[25], [65], [10], [41]
Parietene	78 g/m^2	1.5 mm	Standard	38.9 N/cm	0.9 $\pm$ 0.1 N/mm	-	-	19.9%	[25], [1], [10], [142]
Fluoropassiv	-	Macro	-	-	-	-	-	-	[65]
Gore-Tex	Heavyweight	0.003 mm	Heavyweight	16 N/cm	-	-	-	-	[1], [5]
Mosquito mesh	34 g/m^2	2 x 2.3 mm	Ultralight	20 N/cm	-	-	-	-	[40]
Serapren	116 g/m^2	0.08 - 0.1 mm	Heavyweight	-	-	-	-	-	[10]
Prolite	85 - 90 g/m^2	0.6 - 0.8 mm	Standard	138 N/cm	-	138 $\pm$ 2.3 N/cm	-	-	[1], [10], [143]
Optilene	36 - 48 g/m^2	1 - 3.6 mm	Lightweight	58 N/cm	191.1 N/cm	-	-	10.11 $\pm$ 3.07%	[1], [10], [41], [139]
Atrium	92 g/m^2	0.8 mm	Standard	56.2 N/cm	-	-	14 N	-	[1], [10], [140]
BardSoft	44 g/m^2	2.5 mm	Lightweight	-	124.53	-	-	-	[10], [139]
Mersilene	33 - 40 g/m^2	1 mm	Lightweight	19 N/cm	-	-	15.8 N	-	[1], [10], [140]
DualMesh	320 g/m^2	0.003 mm	Heavyweight	157.7 N/cm	137.59 N/cm	97.8 $\pm$ 7.2 N/cm	-	45.9%	[10], [143], [142], [139]
MycroMesh	Heavyweight	0.0025 - 0.3 mm	Heavyweight	-	-	-	-	-	[10]
AlloMax	-	-	-	23 MPa	-	-	26.2 N	-	[144]
AlloDerm	-	-	-	128.4 N/cm	18.2 N/cm	-	-	-	[142]
Veritas	154.2 g/m^2	-	Heavyweight	29.9 N/cm	10 N/mm	128.6 $\pm$ 8.52 N/cm	-	-	[145], [146], [142]
SurgiMend	-	-	-	432 N/cm	-	432.4 $\pm$ 14.19 N/cm	6.4 %	-	[144]
Permacol	-	-	-	66 N/cm	58.3 N/mm	-	13.1 %	-	[144], [142]
Strattice	-	-	-	18 MPa	58.3 N/mm	270.5 $\pm$ 48.91 N/cm	9.6 %	text	[144]
XenMatrix	-	-	-	14 MPa	-	377 $\pm$ 41.34 N/cm	-	-	[145]
Flex HD	-	-	-	10 MPa	-	-	21.2 %	-	[144]
Surgisis	-	-	-	4 MPa	-	-	-	-	[142]
Proceed	-	3.5 x 2.5 mm	-	56.6 N/cm	129.72 N/cm	52.6 $\pm$ 5.1 N/cm	-	-	[1], [139], [143]
Sepramesh	217 g/m^2	Macro	Heavyweight	52.6 N/cm	-	-	-	18.1%	[139], [50]
UltraPro	28 g/m^2	2 - 4 mm	Lightweight	55 N/cm	4.3 $\pm$ 0.4 N/mm	35.5 $\pm$ 1.7 N/cm	-	14.76%	[25], [1], [142], [143]
Dynamesh	78 g/m^2	1 mm	Standard	11.1 $\pm$ 6.4 N/cm	0.3 $\pm$ 0.1 N/cm	-	-	-	[25], [1], [41]
Ti-Mesh	16, 35, 65 g/m^2	$>$ 1 mm	Ultra and lightweight	12 N/cm	-	-	-	-	[1], [10]
Vypro, Vypro II	26.8 g/m^2	1 -4 mm	Lightweight	t16 N/cm	-	-	15.8 N	-	[1], [142]
Parietex	38 g/m^2	1.8 x 1.5 mm	Lightweight	-	-	-	3.5 N	-	[1], [10]

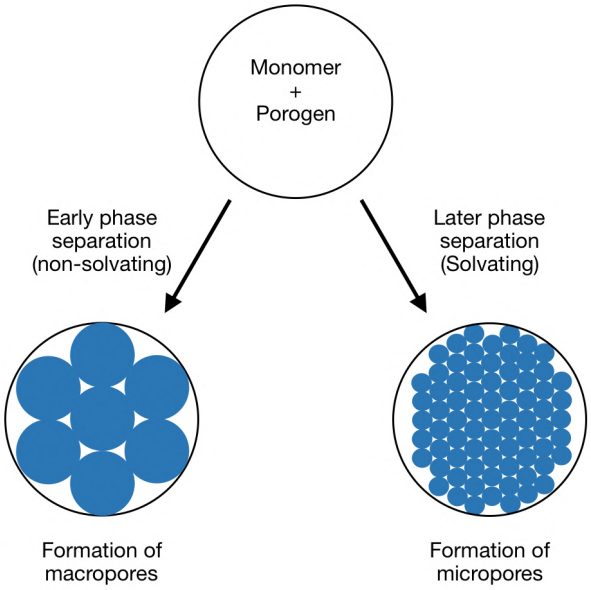

Figure 2.2: Schematic representation of a porogen process.

2.4.1 Porogen criteria selection

The main parameters by which a porogen is selected are based on the molecular size of the solvent, the alkyl chain length and the solubility parameter [149]. This last parameter is shown to cause different performances on the polymers including the morphology, the pore size, the thermal decomposition temperature among others [150]. There exist three types of solubility parameter values [149]:

1. Hildebrand solubility parameter: Which is used in cases where solutions do not have molecular polarity of specific intermolecular interactions.

2. Two-component solubility parameter: Where the physical and chemical components matter and the its use is in solvents with lower molar volumes.

3. Hansen's three-component solubility parameter: For solvents with greater molar volumes.

2.5 Manufacturing

The manufacturing process of prosthetic meshes is important since the structure, properties and other characteristics can be modified. As mentioned above, the creation of a mesh depends on factors and properties such as: pore size, weight, type of structure, stiffness, tensile

strength, etc. The meshes for hernia can have 2 types of configuration: monofilament or multifilament. According to the literature, multifilament meshes are structured by a small pore size, approximately 10 um, instead a long pore size (approx. 2 mm) is better for a monofilament mesh, since it has been proven that pore size affects [41]. From this principle, the development of meshes has had many variants in terms of fiber arrangement, from: knitted, warp-knitted, woven and non-woven [34], different brands such as Marlex, Ultrapro, Prolene, Vypro, Proceed, Vycril, etc., generate their meshes with this type of configuration. One aspect that highlights us Rastegarpour [15], is the difference between knit and woven (figure 2.3), where it mentions that the knitting process is based on a series of filaments are wound with each other, also to have more porosity, however the woven process is based on filaments that go between crusaders and have the same mechanical properties in all axes of the mesh. An important point is that these structures possess anisotropic properties.

With regard to the warp-knitted process, this is a process derived from knitted. There are two processes: warp knitted and weft knitted [41]. In the first, the mesh is made up of an interlacing of threads generating a braid structure [151]. Currently, most commercial meshes have a warp knitted structure because they have a good response to the treatment of hernias by having a large pore size and good elasticity, and they are not susceptible to loss of material or structural strength [34]. In weft knitted, the mesh is made up of a single filament, which is interwoven with other filaments by the center of the knot perpendicularly, in addition these structures are more narrow and deformable, unlike warp knitted [152]. According to Baylon et al. [1], these types of structures have optimal mechanical properties such as elasticity, tensile strength, porosity, etc., which allows them to have a great adaptation to the natural movement of the human body and avoid complications to the patient.

In the literature several authors mention the most used system for the production of knitted structures, which is carried out with a Tricot machinery, which has an E28 gauge. In the same way there are other mechanical systems such as Raschel (gauge E40) or flat-bed, which produce warp and wetf knitted structures. The main difference between these machines is the gauge, which in the case of Tricot is expressed in needles per square inch (E), while in Raschel it is a needle by two inches, they are also tend to have bolts larger than flat-bed because we want to ensure that the filament goes inside and not below the bolt [153]. The mechanical properties are associated to the structure, this is why manufacturing process in very important, so that distance, porosity, diameter, handling are essential to have a mesh with good functionality and good properties.

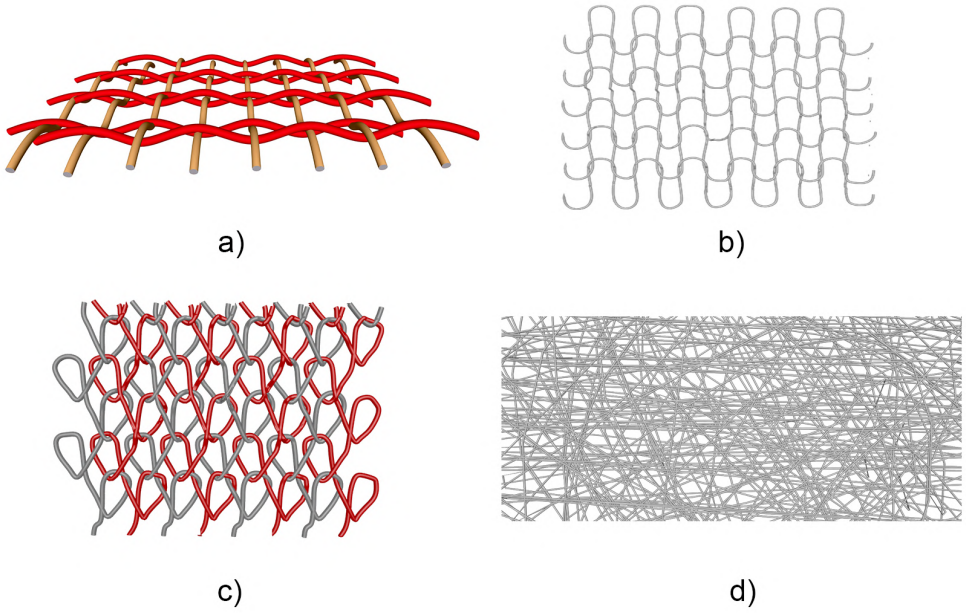

Figure 2.3: Surgical mesh structure depending on manufacturing process. a) Woven structure b) Weft knitted structure c) Warp knitted structure d) Non woven structure.

The non-woven process differs in how the yarn is processed, since in this type of structure there is no order but an orientation. The fibers are distributed throughout the joint or crosslinked mesh and second layers can be placed to improve the properties thereof. A problem with this type of structure is that the fibers are ”poorly” connected to each other so they are more porous than other forms of machining. One way to improve this is to join the fibers by some method such as: spot bonding, print bonding, spray bonding, stitch bonding [154].

2.6 Biocompatible materials

2.6.1 Polycaprolactone

This synthetic biodegradable polymer is considered part of the polyester family with elastomeric properties. Polycaprolactone (PCL) is a hydrophobic, semicrystalline polymer with a 69% of crystallinity (see table 2.6), this degree tends to decrease with increasing the molecular weight [155, 156]. Its physical-chemical, rheological, viscoelastic and mechanical properties depend on its crystallinity and molecular weight, also posses excellent biocompatibility, flexibility and thermoplasticity. This characteristics make PCL a suitable material for medical applications, for example, its use in tissue enginnering and drug delivery systems has been growth in recent years but also in non medical fields as food and environment. Thanks to this, it has achieved its certification by the FDA (Food and Drug Administration) and for the CE

(European community). [157].

PCL has a great solubility (at room temperature) in many organic materials, such as, benzene, chloroform, dichloromethane, toluene, carbon tetrachloride and cyclohexanone. Its solubility is lower in acetone, dimetilformamide, ethyl acetate and 2-butonate. Finally, is insoluble in water, alcohol, petroleum ether and diethyl ether [155].

The biodegradability of PCL can be realized by different methods. It can be by environment or into the body by reactions. The degradability of this material depends on its crystallinity, molecular weight, shape, among other factors. Generally, PCL takes from several months to 2-3 years in degrade depending on the media, for example, inside the body the process is performed by enzymatic degradation and take place by the action of lipase and esterase enzymes. It is necessary to consider factors as pH who has influence on the degradation rate. In this process the amorphous phase is the first part to be degraded causing an increase in the crystallinity [158, 159].

Actually, the use of PCL has grown in the medical area. The production of medical devices, sutures and prothesis has been generated. In recent investigations, the use of PCL in hernia repair has growth. Barbora et al., elaborated PCL nanofibers, which were added to a polypropylene (prolene) mesh and they found an improvement related to the metabolic activity and the proliferation on fibroblast, which allowed the formation of a tick film of fibrous tissue around the implant, moreover, the formation and maduration of collagen helped to the formation of microvessels and to have a scar with less fat tissue [160]. Other authors like Martin et al., confirmed that PCL nanofibers can help and improve the metabolic activity, proliferation, adhesion and viability of fibroblasts, furthermore, these nanofibers can act as carriers, in this case carry thrombocytes for regenerative tissue [161]. In additon, Hansen et al., studied PCL meshes with mesenchymal stem cells and found out that these meshes have excellent biocompatibility and a reduction in post-operative drawbacks according to the in vivo assays [162]. However, the use of PCL with other polymers, such as poly(lactic-co-glycolic acid) (PLGA), polyethylene glycol (PEG), polyethylenimine (PEI) and even organic materials can enhance its mechanical, biological and thermal properties to produce nanoparticles for delivery systems. [158].

2.6.2 Hyaluronic Acid

Hyaluronic acid (HA) is a natural biomaterial which is not sulfated, classified as an unbranched polyssacharide composed by D-gluconic acid and N-acetyl-D-glucosamine with β

Table 2.7: Physical properties of polycaprolactone [156]

Property	Units	Conditions	Value
Physical state	-	Semicrystalline	-
Degree of crystallinity	%	DSC	69
Unit cell	-	- X-ray diffraction	Orthorhombic: 2θ peaks at 21.4, 22 and 23.4
Measure density	g cm^{-3}	X-ray diffraction	1.094-1.200
Elongation	%	-	700
Glass transition temperature T_g	K	DSC	201
Melting temperature T_m	K	DSC	331
Heat of fusion ΔH_f	kJ mol^{-1}	DSC	8.9

(1-4) interglycosidic linkages (figure 2.4) [163, 164]. The polymeric chain of HA is connected by β -1,3 and β - 1,4 bonds between the glucosamide and gluconic acid and this can produce different molecular weights. The weight will give different characteristics to hyaluronic acid. In low molecular weight (LMW), HA promotes the adhesion and proliferation of endothelial cells, while in high molecular weight (HMW) HA functions are completely inverse, inhibits cell proliferation, migration of the vascular endothelial cell [165].

HA is negatively charged and has hydrophilic behavior but when is dissolved it develops hydrophobic faces due the H-bonds created by the interactions with water between carboxy and acetoamide groups. This negatively characteristic comes from anionic charges fixed to the polymer chain, which help to create space between the polymeric structure through which cells can move, promoting the proliferation and migration of these [166]. Due the nature of HA cell migration is facilitated. According to different authors, stem cells can migrate and proliferate from their original niches to distant sites, also, plays a significant role in differentiation process and inflammation. The main receptor CD44 is involved in cell-cell and cell-matrix interactions and when this one is blocked or inhibited the healing process is reduced [163, 167, 168] .

Degradation of hyaluronic acid can be accomplished by different methods. One of them is by hyaluronidases (HYALS), i.e., consist in a degradation based on enzymes including HYALS and PH20 which breaks bonds on gluconic acid and glucosamides. HYALS 1 to 3 are present at acidic pH, specifically HYAL1 is only active at low pH levels, while PH20 is active at neutral pH. Another degradation method is by nonspecific pathways represented by oxidation-reduction process, including species as superoxide, hydrogen peroxide, nitric oxide and others, but excessive reactive oxygen species contributes to a proinflammatory status by

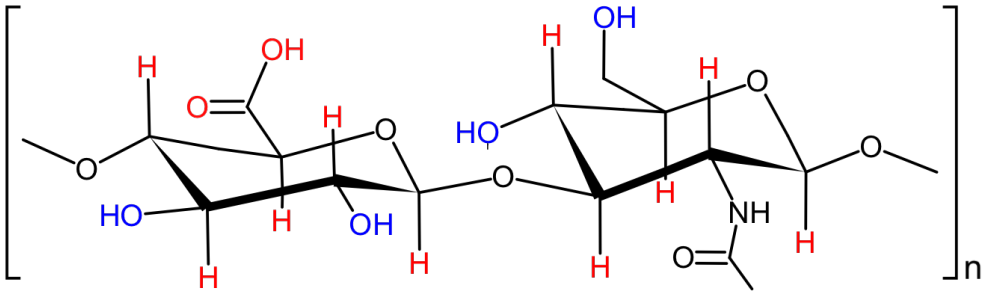

Figure 2.4: Chemical representation of the polymeric chain of hyaluronic acid. The hydrogen atoms represented in red contribute for the hydrophobicity due the creation of hydrogen bonds when dissolved. The left side represents the carboxyl group composed by gluconic acid, while the right side represents the N-acetyl-D-glucosamine group.

the oxidative degradation of hyaluronan [169].

Its use in diverse areas has been growing in the recent years, from pharmaceutical, ophthalmology, therapeutics, cosmetics and many more. In therapeutics is one of the most current biomaterials used endorsed by the FDA. The creation of scaffolds, hydrogels, drug delivery systems and protector layers are utilized to avoid adhesion between organs and tissues, as a local analgesic treatment, and as a coating on skin wounds. In regenerative medicine HA hydrogels works as temporary substitute for the extracellular matrix giving strength and support to cells. In hernia repair commonly act as a barrier between the mesh and viscera. Gillion et al, studied a case control with the use of Ventralight ST mesh with sepramesh (HA/carboxymethylcellulose (CMC)) and the results showed minor complications and no recurrences after one year followed-up. This is attributed to the layer of HA/CMC, which prevents the formation of adhesion and visceral erosion in where bowels floats, separating the intestines and allowing adhesion-free. [170]. Due to this property, hyaluronic acid has been used in the medical area as an anti-barrier material, however, HA has a widespread of uses. Its use in differentiation and growth of stem cells is increasing. Many authors have used HA as a medium to obtain bone marrow, adipose, neural and osteogenic stems cells [171, 172, 173, 174]. The results obtained by HA helps in wound healing issues by reducing inflammation, enhancing granulation formation, obtaining high proliferation rates and promoting bone regeneration. Table 2.7 shows different uses of HA exploiting the viscosity that has.

Table 2.8: Uses of hyaluronic acid in diverse applications [163].

Viscosurgery	Viscoaugmentation	Viscoseparation	Viscoprotection
Helps by keeping tissue in place and preventing displacement. Also, is used to preserve the operative space and to protect the tissue layers from damage.	Intracellular space of the connective tissue is filled with HA for skin, vocal cord and sphincters augmentation in different treatments.	Generally, its use in this application comes from hydrogels and membranes, due HA does not interact with thrombocytes and proteins prevents adhesion between connective tissue surfaces.	Its primary function is to maintain the extracellular space and hydrate the structure for nutrient transport. Also, promotes wound healing due cell migration.

2.6.3 Vitamin E

Vitamin E is a component found in different kinds of foods and oils, as well in the human body. This is a hydrophobic material that it can be classified according to its chemical structure into tocopherol and tocotrienol [12] and these are related with its isoforms ($\alpha-$, $\beta-$, $\gamma-$, and $\sigma-$) which provide different properties to vitamin E. Of these eight, $\alpha-$ tocopherol is the one that has the most relevance in the human body, unlike the other isoforms, since the lasts have faster metabolic activity and therefore, they are excreted outside the body quicker. Because of this, $\alpha-$ tocopherol can be found in higher concentrations against the other kind of isoforms. In the serum and red blood cells $\alpha-$ and $\gamma-$ tocopherols can be found, while $\beta-$ and $\sigma-$ are found in the plasma in small concentrations [175].

It is well known that vitamin E has antioxidant properties in oxidative stress and lipid peroxidation which help to prevent diseases and physical conditions such as cancer and aging. This process occurs by a reduction of oxygen species due to the release of hydrogen atoms in the hydroxyl groups (-OH) in the aromatic ring of the polymer chain. This mechanism allows the liberation of free radicals which becomes unreactive, however, this depends on the type ox the oxygen specie due not all species can be inhibited as lipoxygenase, cyclooxygenase, cytochrome P450, and hypochlorite [176, 177]. Also. anti-inflammatory properties have been related to vitamin E. England et al., studied these properties response of α-tocopherol in a group of men. According to them, this isoform of vitamin E increases the inflammatory cytokine production, however, they highlight that this production depends on the genotype of each individual and the oxidative stress capacity [120]. However, other isoforms ($\beta-$, $\gamma-$, and $\sigma-$) have similar properties. As mentioned above the most popular and investigated form of vitamin E is α-tocopherol but some research indicates that γ, and σ types are better in anti-inflammatory and antioxidant properties [178, 179].

It is commonly used for wound dressing and recently for drug delivery systems due

to these properties. In addition, its use in the repair of hernias and reduction of postoperative complications has been poorly investigated. Gil and coworkers investigated the anti-inflammatory response of α-tocopherol as a coating on a polypropylene (Prolene) mesh and they found that the composite mesh had lower values in production of macrophages and lower foreign body giant cells (FBGC). They inferred that this was provoked by all tocopherols which were able to inhibit pro-inflammatory molecules (IL-1β) [122]. Other studies have been used Vitamin E to avoid postoperative intraperitoneal adhesion formation. In the study, authors induced adhesion and then administrated vitamin E, olive oil and human amniotic membrane (HAM) after the surgical procedure to rats. They found that vitamin E has the lower scores in adhesion study, also it has mild values compared with HAM, however, De La Portilla, et al., did similar studies and found that Vitamin E was not sufficient to reduce adhesion formation when is intramuscular administrated but effective in intraperitoneal administration, thus, result can vary according to different studies [180, 181].

2.7 Stem cells

Stem cells today represent an alternative to problems in regenerative medicine. These cells are capable of self-regeneration and producing new cells capable of transforming into multiple cell types [8]. With this, problems such as tissue, organ, congenital defect and disease repair can be attacked, which is why regenerative medicine has great relevance in the use of stem cells [9].

An important part in the use of stem cells is cellular potential, which is defined as the ability of the cell to differentiate into a specific type of cell with better and greater characteristics. These are categorized into stem cells: pluripotent, multipotent, oligopotent and unipotent totipotent [182].

Thanks to the fact that we can differentiate the stem cells in different types, their use in the area of tissue engineering has been of great relevance for researchers. The use of scaffolds represents a new aspect for cell growth and proliferation since the body requires interaction and integration of tissues and cells [183]. Given this new developments have been implemented in this area to get the most out of it.

An area where stem cells can be considered as ”recent” is the treatment of hernias. Currently different types of cells obtained from different sources such as adipose tissue and bone

marrow have been used to implement them in hernia meshes that help in the repair of abdominal wall, this because the current meshes present certain disadvantages which can be solved with the Use of these cells.

Different authors such as Zhao [107], Altman [184] and Cheng [91], they used adipose tissue stem cells in polypropylene meshes and swine dermis in order to reduce problems in the inflammatory response, improve the biocompatibility of the mesh with the body and reduce tissue adhesions, however these are not the only ones problematic to combat in this area, most of these authors used animal models of rabbits to perform the analyzes. Dolce [185], investigated the use of stem cells derived from bone marrow in a commercial mesh known as Vycril seeking to reduce adhesions, improving biocompatibility and avoid post-operative complications, although Gao [63] in 2014 mentions an interesting part which is that the cells can affect the biocompatibility with the tissue because these cells, which adhere as a coating to the mesh cause a suppression of cytokines which help this process, however this does not detract from the qualities of the stem cells, since they are excellent for reducing the inflammatory response as indicated by the studies of Blazquez [186], by creating an anti-inflammatory environment by macrophage polarization, using a polypropylene mesh, as well as other studies which are shown in table 2.8. Liu and coworkers elaborated an autologous bionic tissue based on PLGA scaffold with the addition of mesenchymal stem cells (MSCs) and were compared with control PLGA. These cells helped in the production of collagen, elastin and hyaluronic acid, which construct new collagen fibers and vascularization for native tissue in the affected area. Also, MSCs reduced the inflammatory response of PLGA by increasing the number of macrophages M2 [135]. By using stromal vascular cells, Guillaume and coworkers mentioned that it can be possible to obtain different lineages of stem cells (mesenchymal, hematopoietic, endothelial) and also, the stromal cells allowed the regeneration of muscular fibers. In their study these cells was used to develop a biologic coating for hernia mesh, obtaining a well acceptance by the animal models and decreasing in short-term the vascular growth during days 10-21, however, according to the study these cells apparently died or migrated after 21 days [187].

Because this topic is gaining ground in the medical area, few studies have been conducted on stem cells applied in hernia mesh, however, the results are promising since they have helped to improve negative factors of synthetic and biological meshes. Currently, the use of scaffolds, as well as the implementation of fibroblasts or cytokines for the growth, differentiation and deposition of stem cells is becoming a more striking area thanks to the advantages they possess, although despite this their use still depends of strict regulations.

Table 2.9: Overview of different stem cells used in hernia mesh

Mesh	Source	Differentiation	Type of hernia	Outcome	Author
Polypropylene	Adipose derived stem cells from rats	Adipocytes, osteocytes and chondrocytes	Inguinal	Decrease in inflammation response	[107]
Polypropylene (Surgimesh)	Human adipose/Murine bone marrow	-	Incisional	Anti inflammatory environment	[186]
Polypropylene	Adipose derived from rabbit	-	Hypogastric	Improve biocompatibility, reduce inflammation and tissue reaction	[188]
Bovine pericardium (Veritas)	Bone marrow from rats	Adipocytes and osteocytes	Ventral	Improve of infection resistance, facility incorporation into tissue	[189]
Polyester (Parietex), Copolymer (TIGR) and Collagen (Strattice)	Rat mesenchymal stem cells	-	-	Promotes cell integration and better performance in biologic meshes (collagen deposition)	[184]
Porcine dermal matrix (Strattice)	Adipose derived from rats	-	Ventral	Enhancement in incorporation, vascularity and cell infiltration	[59] [190]
Polyester (Parietex), Copolymer (TIGR), Collagen (Strattice) and PP (SoftMesh)	Mesenchymal stem cells from rats	Monocytes	-	Cell coating on mesh impact immunogenic potential and tissue interactions causing blunted effect	[59] [191]
Polyglacting 910 (Vycril), Ultrapro and Ethicon	Bone marrow stem cells from rats	-	-	Reduction of adhesion, diminish foreign body responde and improve biocompatibility	[59] [185]
Decellularized dermal scaffold	Bone marrow stem cells from rabbit	Endothelial cells	Abdominal wall	Improve cell infiltration and mechanical performance	[59] [192]
Polyester (Parietex), PP (SoftMesh), PP (Marlex), Copolymer (TIGR) and Collagen (Strattice)	Mesenchymal stem cells from rabbit	-	-	A methodology of stem cell coating	[191]
Porcine dermal collagen	Bone marrow stem cells from human	-	Incisional	Improve of biocompatibility and reduction of recurrences	[193]
Decellularized aorta fibers regeneration and better cell infiltration	Bone marrow stem cells from rabbit	Endothelial cells	Inguinal	Prevention of adhesion formation, tissue	[194]
Poly(lactic-co-glycolic acid) (PLGA)	Bone-marrow mesenchymal SC	Endothelial cells	Inguinal	Lower inflammatory response and production of vascularization for native tissue	[135]
Polypropylene-Titanuim	Mesenchymal stromal cells	stromal vascular cells	Abdominal wall	Reduced vascular growth in the short term and well acceptance	[187]

2.8 Clinical cases

An important part in hernia repair are the clinical cases and these can show the behavior of the materials and the response of the body to these, such as chronic pain, inflammatory response, infections, foreign reaction, among others. In addition animal models are not strong evidence that a surgical mesh can work. Most clinical cases are generated in groups with different genders, ages, diseases or circumstances such as pregnancy, obesity, smoking, etc.

According to the FDA a year, 800,000 surgical procedures were performed to repair the damage caused by hernias, while Baylon, et al. [1], reported 20,000,000 procedures per year, which are still increasing.

These procedures are performed with different techniques such as open repair, laparoscopic, May technique, among others. Depending on the type of hernia, the type of repair to be performed is chosen. The procedures that require less operative time and less pain are those made by laparoscopy, since an opening is not made in the human body as open repair does, as it is a method of minimal invasion (Trial, 2019).

Different authors have evaluated the performance of surgical nets and the types of procedures for the repair of hernia combined with different pathologies. In 2003, Courtney, et al. evaluated 120 patients with different types of hernias (60 incisional, 32 umbilical and 28 epigastric), having a group of men (55%) and women (45%) with an average age of 54.6 years. In this study, 22% of patients with umbilical hernia, incarnation or strangulation compared with 8% presented in incisional hernias. On the other hand Omai, et al., I perform an analysis of women with and without pregnancy evaluating the same types of hernia as Courtney et al., But performing laparoscopy and open repair to know if there is a relationship between pregnancy and the risk of recurrence of hernia Here I found that of the 3578 women evaluated in ventral hernia repair, only 267 had a pregnancy with an average of 3 years after repair. Of all these, a recurrence of hernia of 12.5%(448 women) is observed, in which the incisional hernia is the most prone to present this condition and through cox regression analysis it is observed that there is independence of the recurrence with respect to the pregnancy. Other authors such as Kato et al., Studied the behavior of patients with different types of obesity based on their body mass index (BMI). In their analysis they studied 190 patients where the majority were male (97.4%) with a mean age of 52 years, a mean BMI of 26 and an average operating time of 44 minutes. The patients were separated by obesity index: low weight, normal weight, over weight and obesity. The operation time was variable with each of the patients, finding a

correlation between the operation time and the obesity index causing technical complications. In the same way, Kato et al., Stipulates that factors such as hypertension, obesity and dyslipidemia can cause greater difficulty in surgical procedures with obese patients.

The evaluation of prosthetic meshes is a fundamental part in these cases and the problems of recurrence, inflammation or adhesion not only involve the doctor, but also the material to be implanted in the patient and as the body perceives it. Basically these meshes are for commercial use such as UltraPro®, Parietex®, 3DMax®, Mersilene®, among others. Wai, et al., Studied the repair of ventral hernia during pregnancy using a mesh for Parietex® brand hernia made of a composite polymer in a 41-year-old woman with obesity and pregnancy. The results showed that there were no complications with the mesh in post-operative stages or with the woman in the gestation stage, concluding that hernia repair is safe during pregnancy processes.

Chapter 3

Methodology

3.1 Synthesis of polycaprolactone - hialuronic acid - vitamin E membrane

The development of the membranes was carrying out using a mixture of solvents: dimethylformamide and chloroform in a ratio of 70:30. All the process was performed in a constant stirring. The solvents were heat it up at 80°C and 0.5% of citric acid was added. Subsequently, a percentage (10%-12%) of polycaprolactone was diluted in the solution for one hour. After that, a percentage (1%-2%) of xanthan gum was added to the solution. At the same time the temperature was placed at 40°C. Once the temperature was dropped, it was added 0.5% of polylysine according to the design of experiments (DoE). Then, a percentage (0.3%-0.5%) of hyaluronic acid was added. Afterwards, 2% of vitamin E was added in the solution with 10 minutes of difference between them. Finally, 10% of propylene glycol was added in order to obtain a homogeneous solution. The polymeric solution was then deposited on a petri box and dried at room temperature for 48 hours. Figure 3.1 shows the step by step process of the membrane development.

3.1.1 Design of experiments (DoE)

To perform the experimental stage, a design of experiments was developed in Minitab19 (see table 3.2). The model is a Multilevel Factorial Design (MFD) in where three factors will be have two levels and other four factors will be base parameters. The factors that will vary are policaprolactone, hyaluronic acid and xanthan gum, in order to obtain the better solution. Also, the half of the total amount of samples will have polylysine while the other half not. The concentrations for the solutions used are listed in table 3.1. The total amount of samples were sixteen. All the samples were randomized to avoid undesired effects of unknown or

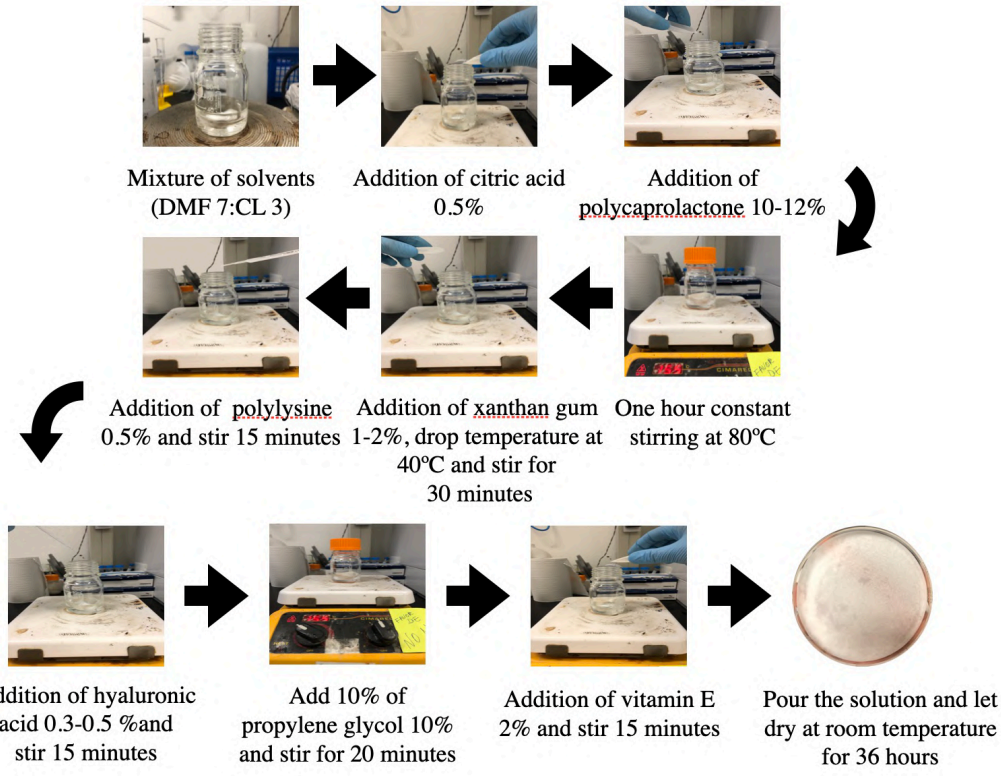

Figure 3.1: Schematic representation of the membrane synthesis (all process was under constant stirring and according the DoE)

Table 3.1: Materials and percentages used during the experimental stage

Paramter	Level	Level
Polycaprolactone	10	12
Hyaluronic Acid	0.3	0.5
Xanthan Gum	1	2
Vitamin E	2	2
Citric Acid	0.5	0.5
Polylysine	With	Without (0.5)
Propylene glycol	10	10

Table 3.2: Parameters used for the development of membranes according to the design of experiments

DoE order	Sample Order	PCL	Solvent (7:3)	HA	Xanthan Gum	Polylysine
1	1	10	DMF-CL	0.3	1	With
3	2	10	DMF-CL	0.3	2	With
4	3	10	DMF-CL	0.3	2	Without
12	4	12	DMF-CL	0.3	2	Without
8	5	10	DMF-CL	0.5	2	Without
5	6	10	DMF-CL	0.5	1	With
9	7	12	DMF-CL	0.3	1	With
13	8	12	DMF-CL	0.5	1	With
16	9	12	DMF-CL	0.5	2	Without
7	10	10	DMF-CL	0.5	2	With
15	11	12	DMF-CL	0.5	2	With
10	12	12	DMF-CL	0.3	1	Without
6	13	10	DMF-CL	0.5	1	Without
11	14	12	DMF-CL	0.3	2	With
2	15	10	DMF-CL	0.3	1	Without
4	16	12	DMF-CL	0.5	1	Without

uncontrolled variables, also it helps to balance the conditions.

3.2 Material characterization

3.2.1 Scanning electron microscopy (SEM)

The SEM (ZEISS model EVO MA 25) was used to characterize the morphology of the membranes. First, the membranes were cut in sections of 1.5 X 1.5 cm. Then, the membranes were exposed and coated with a layer of gold of 5 nanometers to be observed. The equipment was operated with an accelerating voltage of 5.00 kV, high vacuum environment and a work

distance of 10.5 mm. Different magnification were used in order to evaluate the samples (10 μm, 20 μm, 100 μm, 200 μm)

3.2.2 Thermogravimetric analysis (TGA)

The thermogravimetric analyses were carried put using a TGA Perkin Elmer 8000 equipment with a heating rate of 10C/min. To obtain data, the samples were cut in sections of 5 x 3 mm with a weight of 3 mg approximately and submitted to temperatures from 30°C to 600°C using nitrogen as purge gas. The samples remain for 10 minutes at 600°C. All the process took one and a half hour per sample.

3.2.3 Fourier-transform infrared spectroscopy (FT-IR)

A FT-IR (Perkin-Elmer Frontier) equipment with an UATR accessory was used to obtain the chemical structure of principal groups. The procedure consisted in placing the developed membranes of PCL plate on the UATR to achieve a good analysis. The IR spectra were measured in the interval range of 4000 cm1 to 400 cm1 with a resolution of 8 cm1, and by considering an average of 16 scans.

3.2.4 Differential scanning calorimetry (DSC)

To obtain the melting temperatures and crystallinity of all PCL samples a DSC Perkin Elmer 8000 equipment was used. All of the samples were cut in sections of 5 x 3 mm with an average weight of 3.60 mg approximately. After this, samples were encapsulated in aluminum holders with the help of a universal crimper press. The specimens were scanned from 50°C to 100°C with a heating rate of 10C/min, in a nitrogen gas atmosphere without cool process.

3.2.5 X-ray diffraction (XRD)

The XRD measurements of the membranes were carried out using a panalytical empyrean diffractometer with a scanning rate of 2/min and by using copper radiation. Sample by sample was sticked on a rotatory plate and scanned by the system with the following configuration: 45 kV and 40 mA, angle amplitude of 5-70 degrees in $2\theta plane$.

3.2.6 Contact angle (CA)

A data physics system (OCA 15EC) was used to obtain the contact angles of the membranes. The measurements were performed using a syringe, an optical camera and using SCA software. The system consist in dropping water droplet in the membranes with a determined volume capacity of 10 μL and a deposition ratio of 2 $\mu L/s$. The angle between the droplet and the surface is calculated in the software taking account the right and left side of the droplet. 10 measurements were made in each sample to determine an average, to do this the samples were cut in sections of 1 x 1 cm.

3.2.7 Rheological characterization

The rheological properties were carried out by a programmable rotational rheometer Anton Paar (model Physica MCR301), using spindle No. 3912 and a parallel-plate system. The storage modulus, loss modulus, complex viscosity and dumping factor measurements were performed on cylindrical samples of 5 cm under controlled max strain of (0.2%) and frequency (100-0.1 rad/s).

Chapter 4

Results and Discussion

4.1 Scanning electron microscopy (SEM)

4.1.1 Preliminaries

In this stage the 16 membranes made by the DoE information were analyzed, but before analyzing these samples a series of preliminaries was carried out in order to eliminate variables and perform the experimental stage. Firstly, the functionality of the solvents with the polymer was evaluated, creating two solutions: One from polycaprolactone, propylene glycol and the mixture of dimethylformamide with chloroform (DFM-CL) in a range of 7: 3 and another with the same components excepting one change, chloroform by dichloromethane (DFM-DCM) in a range of (80:20). Finally, a sample was made with all the variables to see if there are important changes. The results of these preliminaries can be seen below.

The micrographs (figure 4.1 a,b,c) show the sample of dimethylformamide with chloroform, in which a surface with a uniform pore size can be observed, this due to the good miscibility that solvents have (non-solvating) with polycaprolactone, which allows uniformity in the creation of pores. When performing a histogram (see figure 4.2 a), it was found that the average pore size is at 49.655 μm, however, the distribution of the pore size showed that there are pores of more than 100 μm. Most pores were between 20 and 60 μm in diameter. In addition, it was found that the membrane has a rough surface, the level of roughness will be studied later. Figure 4.1 d,e,f shows the membrane made with dimethylformamide and dichlorometane, which shows a completely irregular surface with different pore sizes, showing a large difference with the DMF-CL membrane. This sample has macropores and does not have uniformity, which is due that DCM has a low boiling point and it has higher solubility properties than chloroform, as can be seen in table 4.1, so this morphology can be

Table 4.1: Physical properties of solvents [195, 196, 149]

Solvent	Boiling Point (°C)	Solubility parameter ($cal^{1/2}cm^{-3/2}$)	Miscibility	Porogenic Type
DFM	62.6	11.79	Good	Non-solvating
DCM	40.0	12.10	Immiscible	-
DFM 80/DCM 20	130.4	10.26	-	Solvating
Chloroform (CL)	61.2	9.21	Good	Non-solvating
DFM 70/CL 30	-	-	Good	-

obtained. The average pore size is 27.742 μm, considering that the sample has pores that are too small, likewise, as observed in the histogram (see figure 4.2 b), the majority of pores are between 10-20 μm but pores from 10 to 100 μm can also be found, demonstrating the size variability of the membrane. The surface also demonstrated the presence of high roughness. The last preliminary analyzed (see figure 4.1 g,h,i) was the sample with all the variables using the DFM-CL solvent mixture because it showed better uniformity in the pore morphology. This membrane showed excellent uniformity and high porosity on its surface with an even more regular pore size, this is due to the mentioned before good miscibility of solvents with the polymer, in addition, the aggregation of materials, such as, hyaluronic acid, vitamin E and propylene glycol seem to give the membrane greater uniformity and stability. It was found that the average pore size is at 32.993 μm, where most of the pores are between 20 and 35 μm according with the histogram (figure 4.2 c) while the largest pores reached up to 70 μm. In the same way as the previous samples, a roughness was found on the surface of the material.

4.1.2 PCL-HA-VE Membranes

After the observation of the preliminaries, it was decided to select the solution of DFM/CL due the better results respecting homogenization and uniform pore size. According to the DoE, sixteen membranes were analyzed, however, 2 more membranes were included, which represent control 1 (PCL-solvents) and control 2 (PCL-Xanthan gum-solvents) in order to compare the main changes. The samples showed different pore sizes, ranging from 6 to 61 μm (see table 4.2). Control 1 and control 2 samples did not showed any significant change in its morphology as it can be seen in figure 4.4, in fact they have almost identical pore sizes and standard deviations, which means that the addition of xanthan gum does not affect the porosity of the material as it can be observed in the histograms (figure 4.3). The morphology and the pore obtained for the rest of the membranes composites was different. Most of the samples show regularity in their morphology regarding the size and uniformity of the pore, although there are membranes with more porosity than others. The size varies considerably only in the

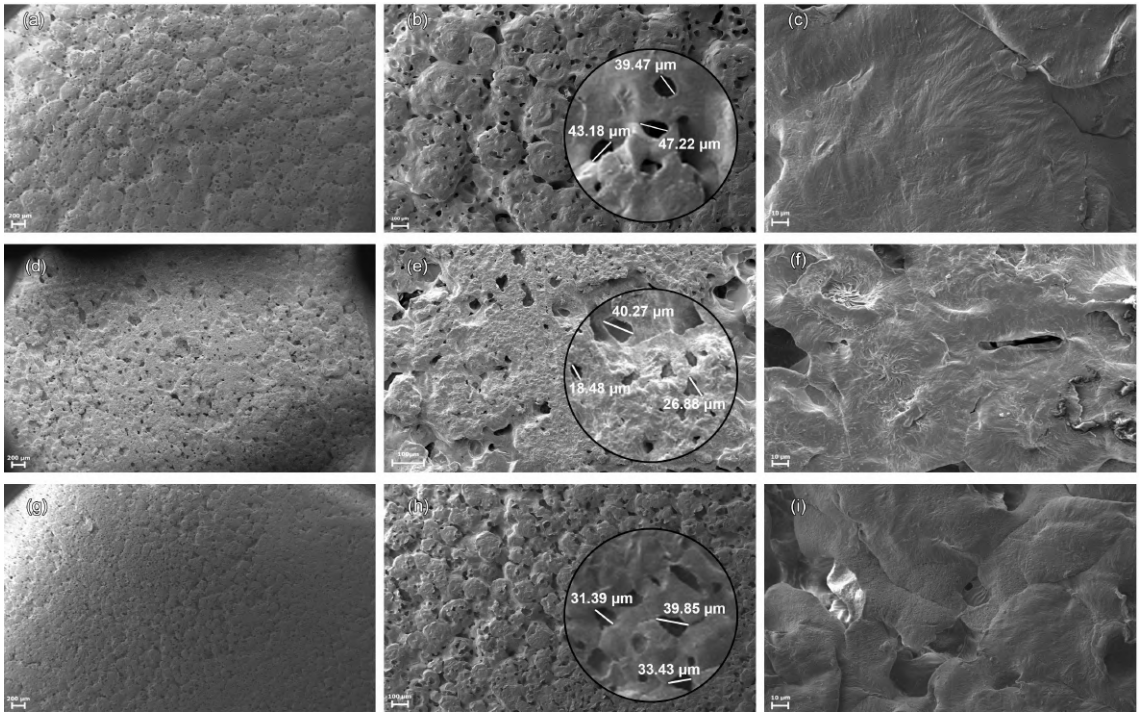

Figure 4.1: Surface SEM micrographs of the composite membranes. (a) Complete view of the membrane, where it can be see the uniformity of the pore size. (b) A zoom view of the morphology of PCL diluted in DFM-CL solvent. A high porosity can be observed on the surface of the material. (c) Roughness of the material. (d) Complete view of the membrane, where it can be see the lack of uniformity of the pore size. (e) A zoom view of the morphology of PCL diluted in DFM-DCM solvent. A high porosity can be observed on the surface of the material. (f) Roughness of the material. This material has the higher roughness, seems to be generated by the mixture of solvents. (g) Complete view of the membrane, where it can be see the uniformity of the pore size because the good miscibility of chloroform and the aggregation of hyaluronic acid, vitamin E and propylene glycol appears to promote this too. (h) A zoom view of the morphology of PCL diluted in DMF-CL solvent. A high porosity can be observed on the surface of the material, also there are regularity in the pore size. (i) Roughness of the material. A high roughness seems to be generated by the compounds.

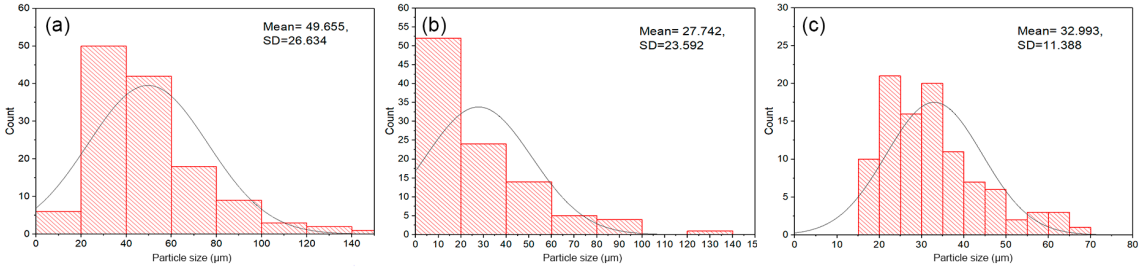

Figure 4.2: Histograms of pore size. (a) Membrane of DFM-CL. (b) Membrane of DFM-DCM. (c) Membrane with all variables (completed)

final samples (13, 14, 15 and 16), since the samples show an average range of 32 to 45 μm, while these have pores below 20 μm. Most show regularity in the pore size distribution (see figure 4.5) up to 60 μm, although there are larger pores but not as regularly. Membranes 7, 8, 9 and 11 (figure 4.6) have similar morphologies, such as uniformity and pore type, however, in samples 9 and 11, greater porosity can be observed on its surface. Proof of this would be that the mean of their pores and their deviations are very similar, between 15 and 19 μm, even samples 1 and 3 are similar in terms of pore size but have less surface porosity. As for samples 6 and 14, these presented different morphologies; the pore does not have regularity, however, they have high porosity. Its surface appears as if it were made up of scales. It can be concluded that these samples were the worst in terms of material conformation. As mentioned above, membranes 13, 14, 15 and 16 presented reduced pores, obtaining pores from 6 μm (sample 15) to 17 μm (sample 16), however, they are still considered macropores. Even so, it is an excellent opportunity that this type of material not only produces pores of more than 30 μm but that it can generate small porosities without the need of methods such as electrospinning [197], only with a variety of parameters and solvents (porogeneity). An assumption to obtain reduced pore would be that at a higher concentration of PCL and HA the pore tends to decrease since it was observed in the control samples that the gum does not interfere in this process. Polylysine, apparently, would not generate significant changes in terms of morphology since the samples with and without the material were uniform, although the pore size in some cases decreased and in others, it increased. The good homogenization and uniformity can be attributed to the good affinity between the reagents and to the solvents that promote more uniform macropore structure [198, 147].

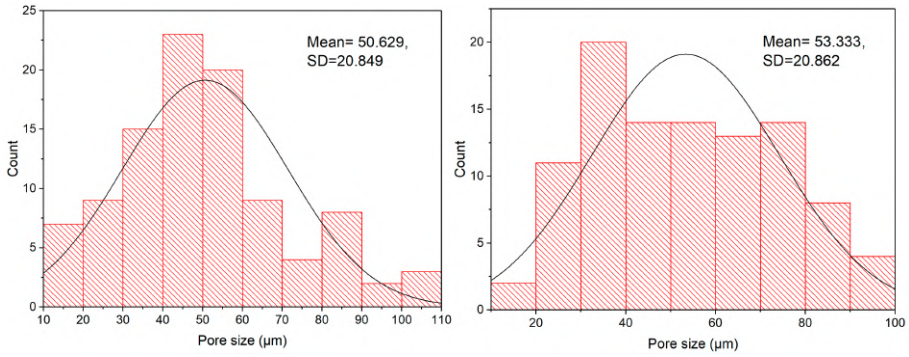

Figure 4.3: Histograms of control 1 and control 2 samples. a) Mean pore size of PCL-DMF-CL membrane. b) Mean pore size of PCL-Xanthan gum-DMF-CL membrane.

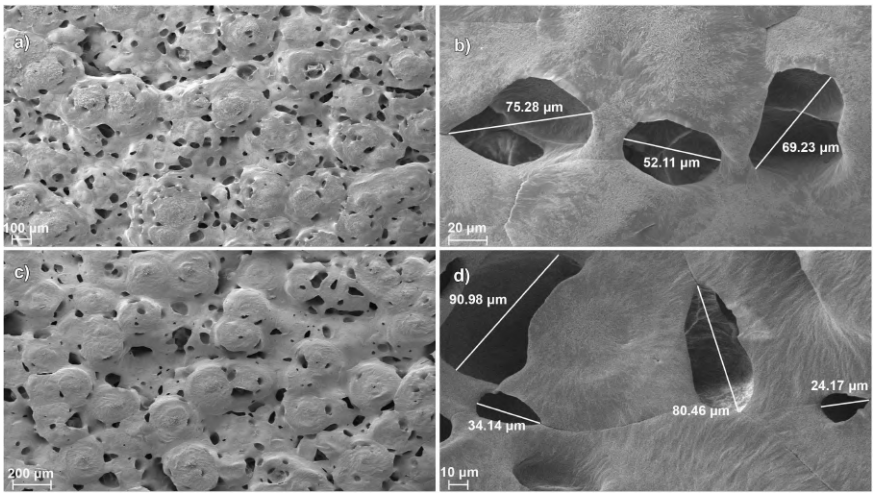

Figure 4.4: Control 1 (above) and control 2 (under) samples. a) Surface porosity of PCL-DMF-CL. b) SEM image showed roughness in the surface and some measurements of pores. c) Surface porosity of PCL-Xanthan gum-DMF-CL. d) Can be seen roughness in the surface and some measurements of pores, and by comparing these two samples can be inferred that xanthan gum does not provokes a change in the morphology.

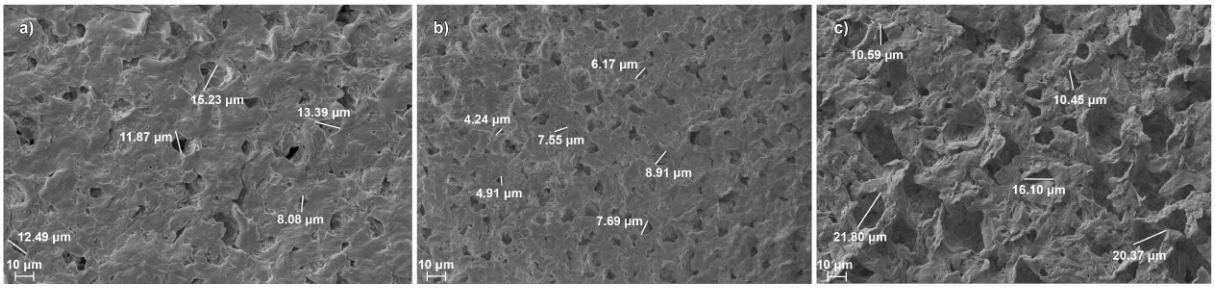

Figure 4.5: Pore reduction of samples 13, 15 and 16. It can be seen a reduction in their pore sizes in almost 90% comparing with control samples. The principal cause can be the that at higher concentration of PCL and HA the pore tends to decrease. a) Sample 13 showed the surface with less porosity with a regular pore size (SD. 3.604). b) Sample 15 presented a large porosity (the highest) on its surface and the smallest pore size, which is around 6 μm. c) Sample 16 has a notorious roughness surface and median pore sizes (around 17 μm), from the three, this one was the sample with the largest pores.

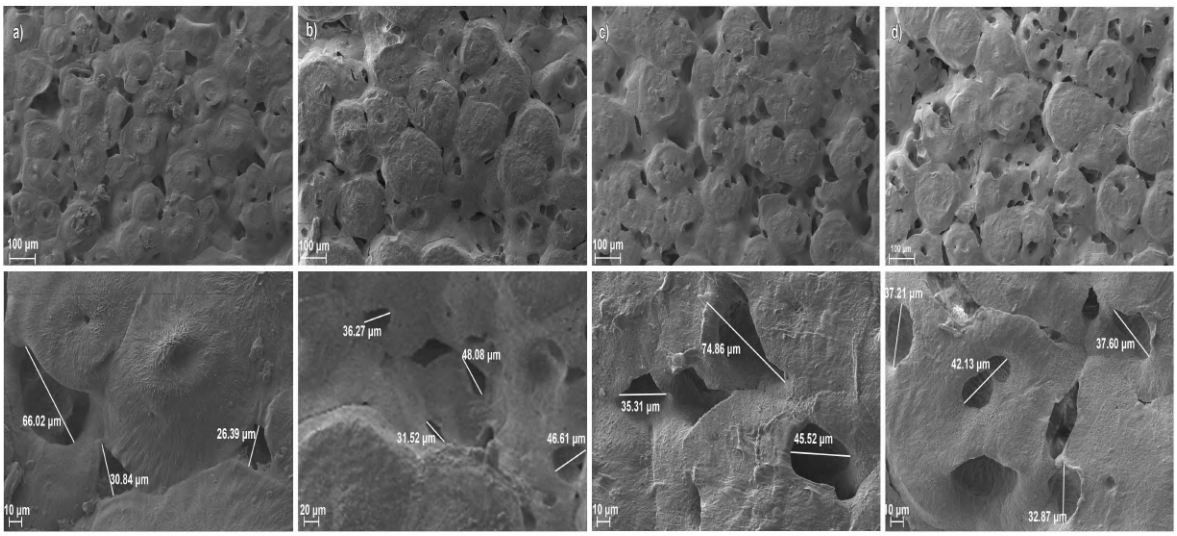

Figure 4.6: SEM micrographs reveals the morphology of the membranes showing a porous surface with regularity. a) Membrane 7 showed less porosity than samples 8, 9 and 11 but it was one of the best porosities. b) Membrane 8 is little more porous than sample 7 and uniformity. c) Membrane 9 showed similarly porosity than sample 8 and a big pore size. d) Membrane 11 has more porosity and similar pore size than sample 7 and 8.

Table 4.2: Morphological results of all the membranes, showing differences in pore size and its standard deviation.

Sample number	Mean pore size (μm)	Standard deviation
Control 1	50.629	20.849
Control 2	53.333	20.862
1	44.102	21.912
2	61.416	29.260
3	35.465	14.744
4	24.691	25.634
5	49.284	24.819
6	28.028	9.985
7	37.480	15.630
8	37.741	15.484
9	44.352	19.145
10	25.385	8.800
11	38.950	17.659
12	32.621	14.028
13	15.059	3.604
14	13.174	7.339
15	6.262	2.294
16	17.234	4.236

4.2 Thermogravimetric Analysis (TGA)

The thermal degradation analysis can be studied by the observation of figure 4.7, which corresponds to sample 1. There are two-step weight loss behaviors presented in the sample. First step loss temperatures are between 190°C-340°C with an inflection point around 285°C with a mass loss of 11% approximately. This behavior corresponds to the decomposition of hyaluronic acid to water and polyssacharides [199, 200], and to the xanthan gum decomposition to water [201]. Second step loss occurs between 340°C-450°C with an inflection point of 410°C corresponding to the decomposition of PCL and vitamin E. PCL decomposes in methyl pentanoate, water and carbon dioxide [198], while a crystalline sublimate ($C_{10}H_{14}O_2$) is obtained by vitamin E [202], also the higher mass loss is located here with 42%.

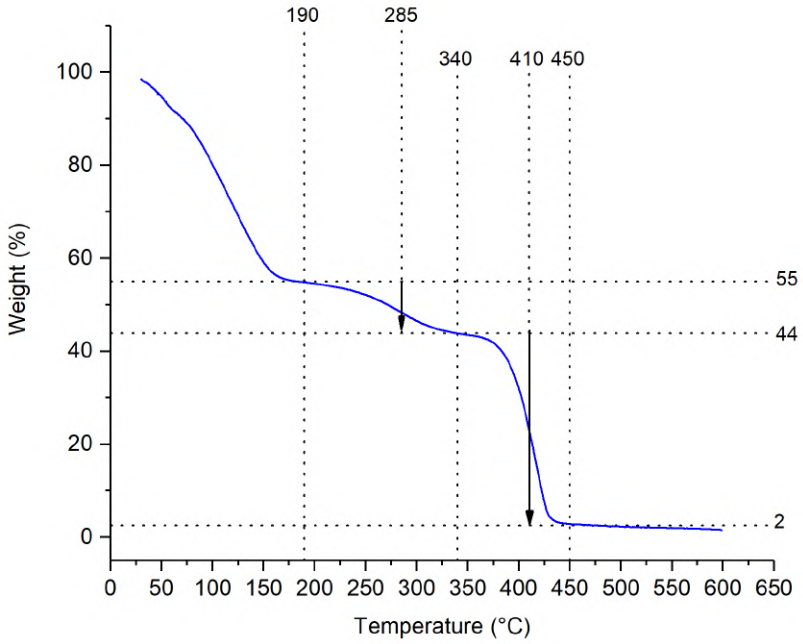

Figure 4.7: Thermogravimetry Analysis of sample 1. It shows the inflection and ranges temperatures for the decomposition of the membrane materials.

The same behavior can be observed in the remains samples as it is shown in figure 4.8, except by control samples 1 and 2 that shown the regular behavior of PCL. The main difference between the samples is the amount of mass loss in the polymer, which varies.

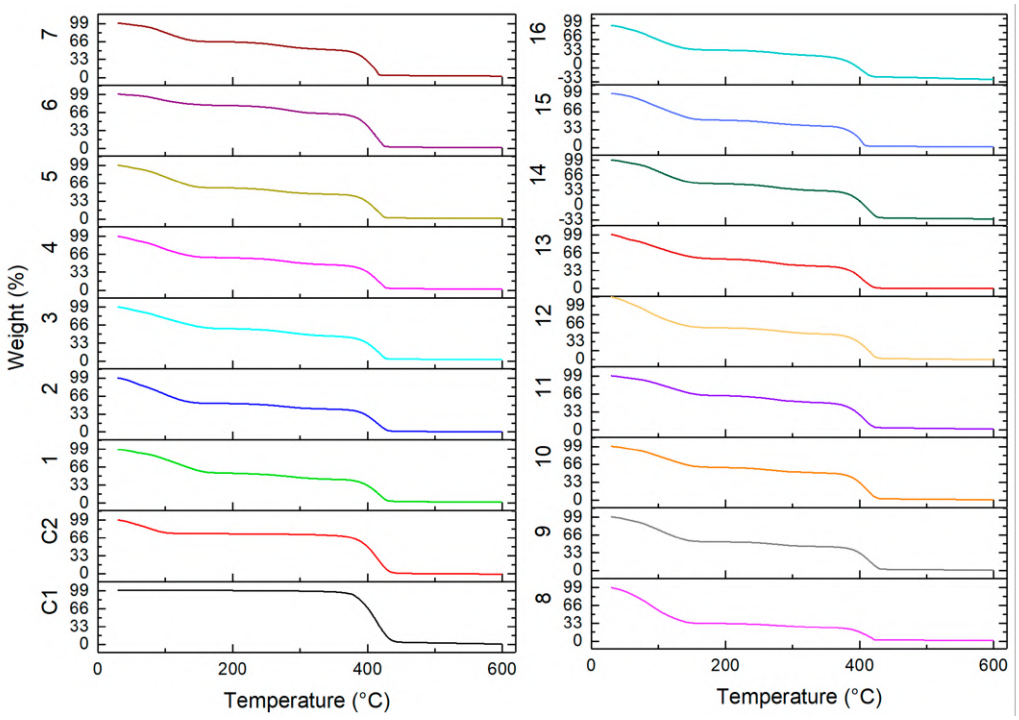

Figure 4.8: Thermograms of control and composite meshes.

4.3 Differential Scanning Calorimetry (DSC)

When analyzing the obtained thermograms, the behavior of the membranes when exposed to a temperature increase was shown, without reaching the point of degradation, since this would affect the crystallization process of the material. The process demonstrated that the samples presented a series of wide exothermic peaks with which the level of crystallinity of the material could be calculated. As seen in figure 4.9, control sample 1 exhibits a melting curve between 53°C and 64°C with an exothermic peak at 61.5°C, which refers to the behavior of PCL with DMF and chloroform, however when including materials at the PCL matrix begins to have a shift, as well as an increase in the width of the thermal curve and a decrease in its amplitude as demonstrated by control sample 2 with the addition of xanthan gum. Samples 1, 2, 5, 6, 9, 10, 13 and 14 are a clear example of how gum affects the shift of the thermal curve since the samples mentioned above have 2% of this material and are found with less shift compared to the remaining samples. In addition, comparing with the SEM results, samples 7, 8, 9 and 11, which were the most stable, revealed a similar onset temperature behavior of around 47°C.

Then, using the equation of $X_c = (\Delta H_m)/(\Delta H_m^0)$, where ΔH_m and ΔH_m^0 are the

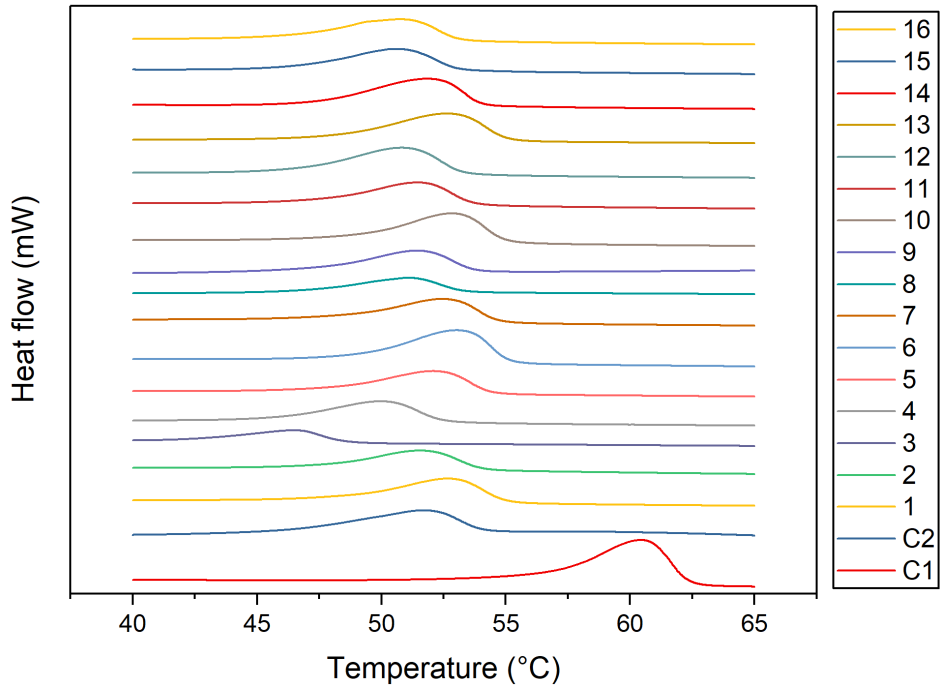

Figure 4.9: Calorimetry Analysis of membrane samples. A shift between the samples can be observed compared to control sample 1, such behavior suggests to be attributed to the percentage of xanthan used in the matrix of PCL.

melting and fully crystalline (139.5 J/g) enthalpies of PCL, the percentage of crystallinity was calculated for pure and composite PCL membranes. These values can be observed in table 4.3. The X_c value for control sample 1 was 41.37%, which is the higher percentage of crystallinity, while the composite samples obtained lower X_c values, between 20% and 30%. The decrease in the crystalline values suggests being attributed to polylysine [203] due it has an amorphous nature and this tends to decrease the crystallinity of PCL.

4.4 Fourier Transform Infrared Spectroscopy (FTIR)

The identification of organic groups (chemical properties) was further confirmed by IR analysis. The presence of PCL, hyaluronic acid, vitamin E, xanthan gum and polylysine was confirmed. This study, showed the vibrational modes of the composite membranes of PCL, as shown in figure 4.10. The IR spectrum shows modes at 3350 cm^{-1} attributed to -OH and -NH groups with a symmetric stretching mode [204, 205], bands around 2837 cm^{-1} and 2867 cm^{-1} correspond to an asymmetric and symmetric stretching modes due C-H hidroxyl (CH=O) groups [206, 207]. The absorption bands at 1721 cm^{-1} confirm the presence of C=O stretching vibrations of carbonyl groups, while band at 1653 cm^{-1} are from C=O symmetric

Table 4.3: Changes in temperature, enthalpies and percentage of crystallinity for pure and composite membranes.

Sample number	$T_{onset}(^oC)$	$\Delta H_m(J/g)$	$X_c(\%)$
Control 1	56.64	61.86	41.37
Control 2	46.09	38.54	27.62
1	48.43	38.09	25.15
2	47.50	29.12	20.87
3	42.35	15.68	11.24
4	45.86	30.95	22.18
5	47.93	33.10	23.72
6	48.76	46.50	33.33
7	48.17	36.58	26.22
8	47.05	21.25	15.23
9	47.38	33.10	23.72
10	49	40.78	29.23
11	47.55	33.41	23.94
12	46.76	38.94	27.91
13	47.93	41.67	29.87
14	47.13	39.34	28.20
15	46.43	32.97	23.63
16	46.36	34.96	25.06

and -NH asymmetric stretching modes. The presence of methylene groups can be observed at 1460 cm^{-1} and 1368 cm^{-1} related to bending modes. The presence of carboxylate (COO^-) groups can be detected at 1417 cm^{-1} associated to symmetric stretching modes. Also, vibrational bands at 1241 cm^{-1} and 1188 cm^{-1} are associated to C-O-C (ester) groups, which represent the crystalline and amorphous behavior of PCL [198]. At the same time, this bands correspond to asymmetric and symmetric stretching modes.

The sixteen membranes shown a similar behavior in their chemical groups compared to control sample 1, however, in samples 2, 4, 8 and 12 there is a decrease in the percentage of transmittance at 1721 cm^{-1}, which may be attributed to the interaction of xanthan gum or PCL due that peak is representative of these materials.

4.5 X-Ray Diffraction (XRD)

Specimen spectograms were obtained by XRD analysis. Assuming that the polymer has a semi-crystalline structure. The PCL control samples were taken by the work of Angel-Sanchez et al. [198] in order to evaluate composite membranes since in their work used same

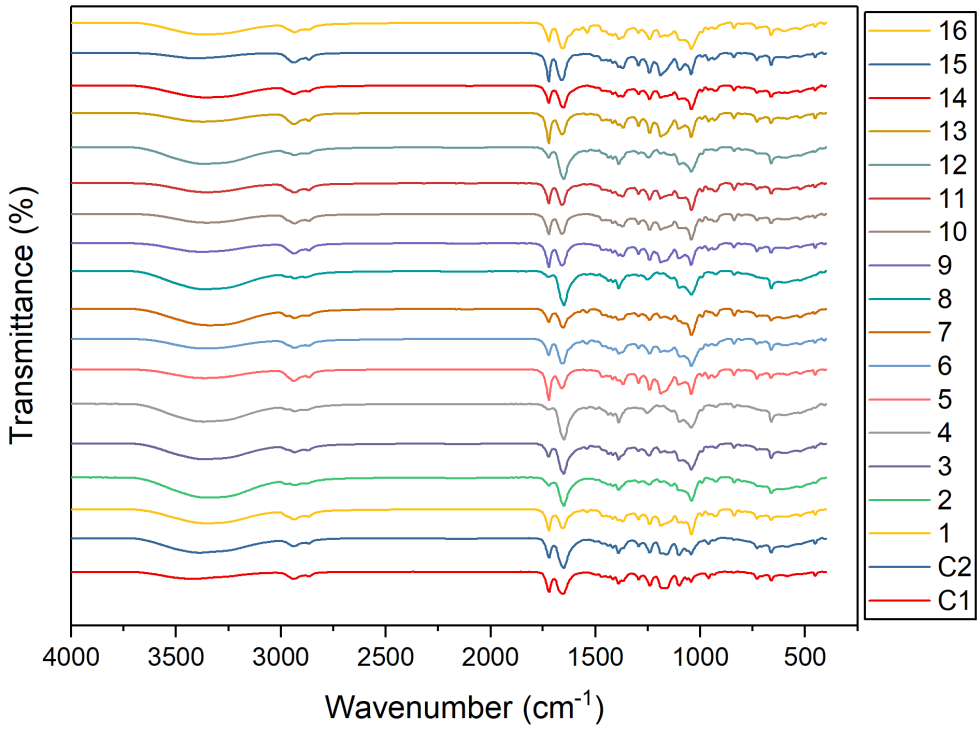

Figure 4.10: FTIR specta of control and composite PCL membranes with detailed vibration bands. The presence of PCL, hyaluronic acid, vitamin E, xanthan gum and polylysine was confirmed.

molecular weight polycaprolactone and solvents, also samples were compared with JCPDS card numbers: 0-1431 and 40-0664. It exhibits two peaks values in the 2θ plane at 21.7 and 24.1. Those peaks correspond to planes (110) and (200), which are characteristic of an orthorombic unit cell [208, 209]. According to this, composite membranes showed similar behavior, in fact these samples reveal a new plane (111) at 22.1 degrees characteristic of orthorombic structure, these are originated due to the intermolecular interactions of hydrogen with PCL chains [210]. In figure 4.11, a shift in the 2θ plane can be observed and attributed to the addition of amorphous materials like xanthan gum, polylysine and hyaluronic acid to PCL matrix [211, 203], also the use of the DMF and chloroform could induce this modification in the polymer chain. Thus, the crystallinity of the material was affected as it could be corroborated with the DSC analysis.

4.6 Contact Angle (CA)

Contact angle values were measured and calculated in order to know the wettability behavior of the control and composite membranes. In figure 4.12, the values of CA are displayed,

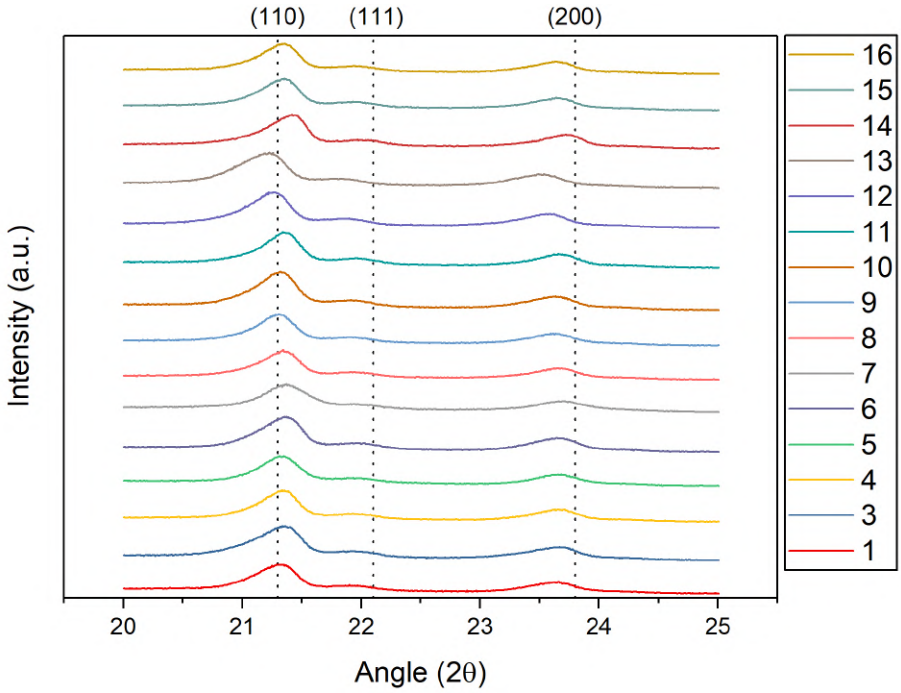

Figure 4.11: XRD analysis of all membranes. Samples from 1 to 16 showed a shift in their angle values.

showing differences in the samples. First of all, control sample 1 shows a hydrophilic behavior with a value of 83.8° ($\theta < 90°$), when it should show hydrophobic behavior according to its nature and to different studies related to PCL [212, 213]. This change in wettability would be produced primarily by the solvents used in the elaboration of the membrane, as it could be observed in the SEM analyzes by showing changes in the morphology of the material, also, studies performed by Prabhakar et al., confirmed that the use of chloroform induces hydrophilicity in PCL due surface energy changes [214], followed by this, the control sample 2 showed an increase in its CA (95.54°) when behaving like a hydrophobic material, so xanthan gum must cause hydrophobicity in the material. In composite membranes, most values are between 71° and 87° showing hydropilicity behavior, but also values of more than 90 can be observed. One reason will be that hyaluronic acid has a natural hydrophilicity behavior, while vitamin E its a hydrophobic material and causes changes in the wettability. Among this, polylysine could be another reason. Some studies indicate natural hydrophilicity behavior due to the amino groups in their chain, however, other studies point out that depending on its interactions, polylysine could provoke hydrophobicity or hydrophilicity [215, 216]. Nevertheless, the behavior between 70° and 90° is favorable, because stem cells prefer this type of environment to be able to adhere and proliferate freely.

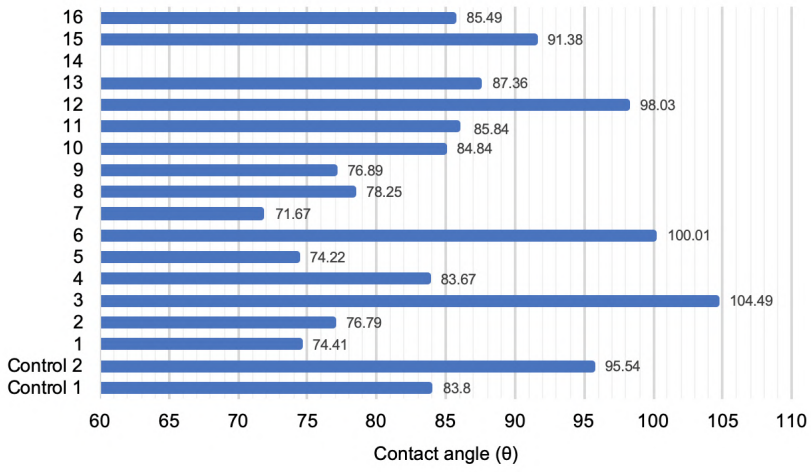

Figure 4.12: Contact angle values of composite and control membranes.

4.7 Rheological Properties

To study the rheological behavior of the samples, storage modulus, loss modulus, complex viscosity and damping factor were compared versus angular frequency (rad/s). All samples were submitted at 37°C, mimicking the internal temperature of the human body. Figure 10 shows the variation in storage (a) and loss (b) modulus. According to this, it can be assumed that PCL membranes are solid-viscoelastic materials due the storage modulus is higher than the loss modulus. In addition, storage modulus exhibit an increase in stiffness of the viscoelastic behavior when xanthan gum is added, on the other hand, at 90-100 rad/s control sample 1 showed shape relaxation which indicates that the addition of gum is improving mechanical behavior. When biomaterials are added to the polymer the values of storage modulus are lower, only samples 2 and 7 exhibit similar behavior than control samples. In fact, 10% polycaprolactone showed higher values in composite membranes. Furthermore, these membranes are well blended because the storage module is below its main component, while poorly blended samples are above the component [217]. Loss modulus which represents the dissipated energy when deformed and the viscous part seems to be stable when adding HA, vitamin E and propylene glycol, meaning low frictional forces in the structure of the material. Note that control sample 1 and 2 show big dissipation energy in their loss modulus at high frequencies, however, most of composite membranes exhibit even an increase in this value at high frequencies. In both analysis can be observed that samples 2, 5 and 7 had the higher values.

In other results, complex viscosity modulus showed a non-newtonian behavior (figure 11.a) due linear decrease in the viscosity when increasing shear rate. All samples followed the

shear-thinning zone with no signals of Newtonian region. Samples with the highest viscosity values are the same as mentioned above (2, 5 and 7). This behavior can be also associated with solvent-polymer interactions or changes in chain rigidity. Figure 11.b shows the relevance of damping factor as the dissipation of the mechanical energy into heat. Note that almost all membrane samples have a slope in their capacity values which starts at 1 rad/s. It can be observed that control samples 1 and 2 have a drastic fall in their capacity, while composite membranes with 10% of PCL have higher values compares with 12% of PCL. Another point to observed is that its damping value (G'/G") is around 0.08 and 0.2 which means that samples are exhibiting an hyper-elastic behavior, this due to strong interaction between the polymer chains causing less internal frictions. As mentioned above the inclusion of biomaterials gives stability to the membrane and promotes higher elastic behavior. Main changes were caused molecular changes in the polymer chain produced by biomaterials and solvents as could be seen in SEM, DSC and DRX. Due to the good miscibility of the polymer in the solvents (DMF and chloroform), porogeneity were able to modify the structure arrangements of the material changing the orientation and the interwine of molecules causing big shear-thinning behavior, also, 10% PCL showed better results as was seen in rheology. As well, as it was seen in DSC and DRX, the addition of solvents and xanthan gum produced shifts in the crystallinity and thermal temperatures of the material which can be related to the lower viscosity capacity but increasing the stiffness.

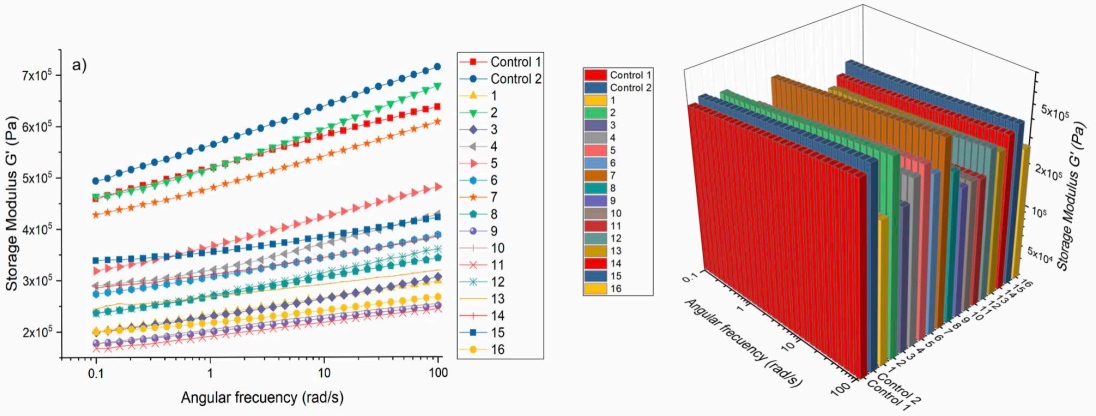

Figure 4.13: Curves of storage modulus vs angular frequency. a)Composite samples 10% PCL. b)Composite samples 12% PCL. c) 3D illustration of the curves behavior.

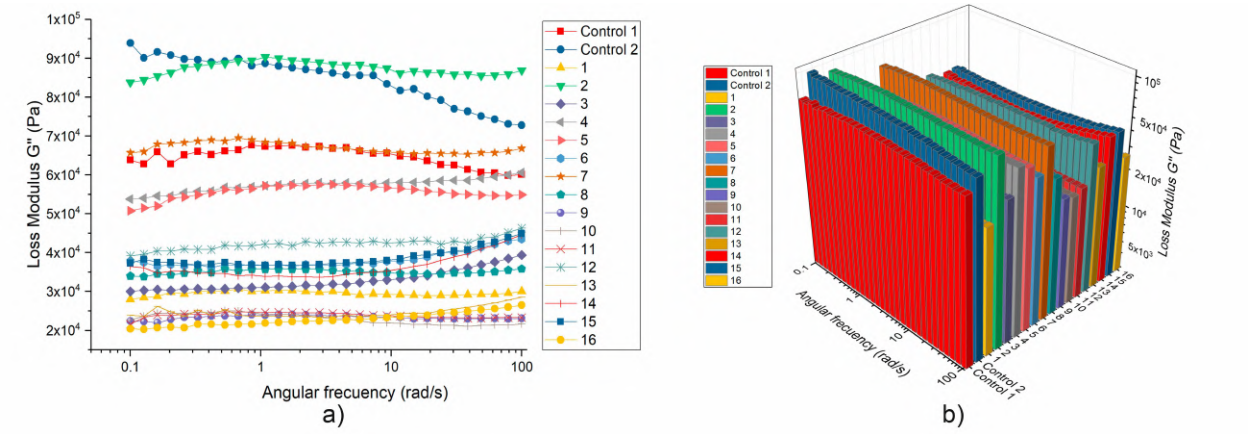

Figure 4.14: Curves of loss modulus vs angular frequency. a)Variation in loss modulus behavior. b)3D illustration of the curves behavior.

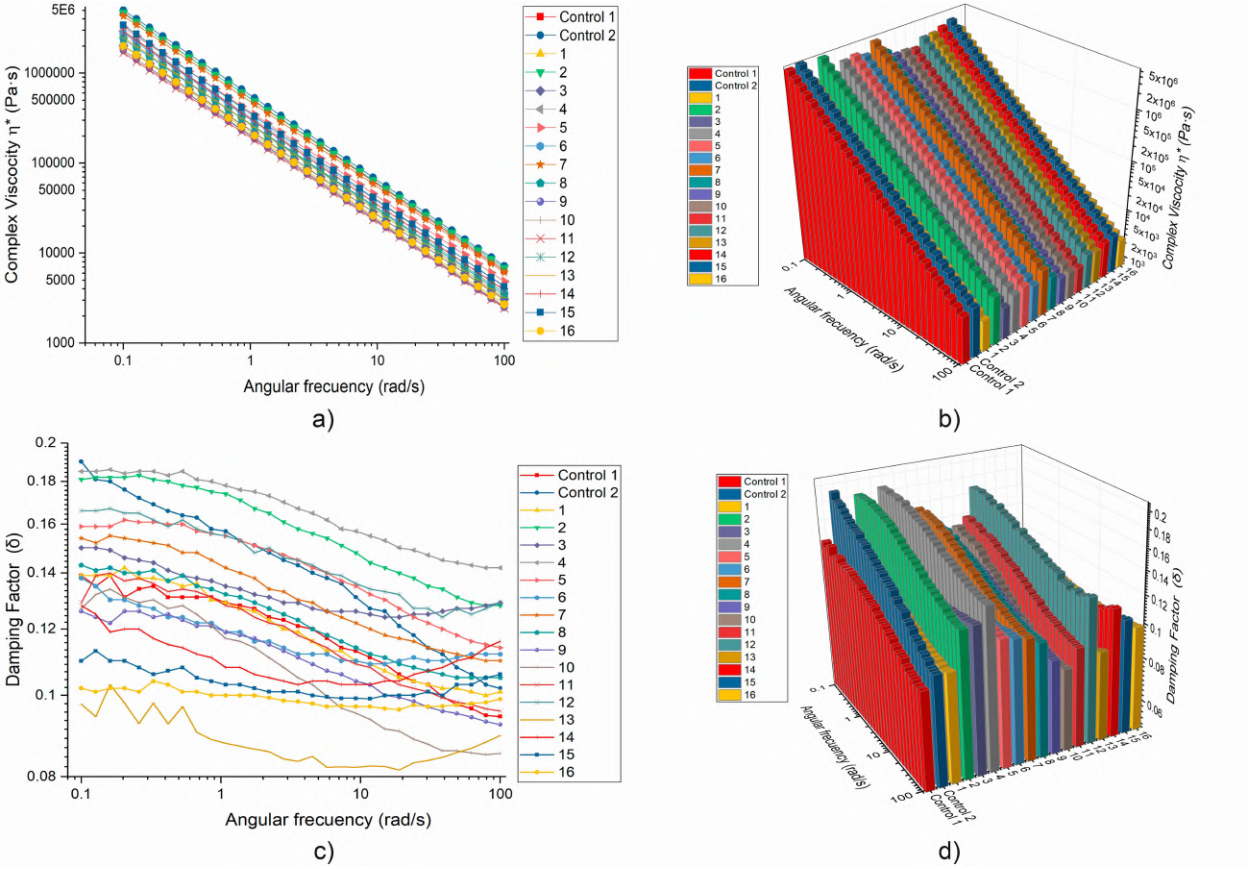

Figure 4.15: Curves of complex viscosity and damping factor vs angular frequency. a)Variation in complex modulus of composite membranes. b)3D illustration of the viscosity behavior. c)Variation in damping factor of composite membranes. d)3D illustration of the damping behavior .

Chapter 5

Conclusion and Future Work

The characterization results provided different behaviors and properties of the coating. By using different type of porogens (solvents) such as chloroform and dimethylformamide, different microstructures and pore sizes could be obtained due to the good miscibility with the polymer. Also, it was seen hyaluronic acid (0.5%) tends to decrease pore size since it was observed in the control samples that the gum does not interfere in this process. Furthermore, the addition of hyaluronic acid, vitamin E and propylene glycol gives uniformity, homogeneity and stability to the matrix, also promotes higher porosity in the surface allowing cell migration by both parts of the coating avoiding post-operative drawbacks. Thermal analysis (TGA) reveals that there exist two-step weight loss behaviors; one involved hyaluronic and xanthan gum decomposition into polysaccharides and water, while PCL decomposes into carbon dioxide, water and ethyl pentanoate giving a big change in mass loss (approx. 40%). However, biggest changes were revealed by calorimetry analisis (DSC). Different crystalline values were found due to the use of polysaccharides and amino acids (xanthan gum, hyaluronic acid and polylysine), since they have an amorphous nature and affect the polymer matrix, also due to the creation of low density hydrogen bonds. Furthermore, there are shifts in their melting temperatures caused by the use of chloroform and dimethylformamide. Wettability variation (hydrophobic/hydrophilic behavior) could be achieved by the inclusion of solvents due to chloroform tends to promotes hidrophilicity by destruction of intermolecular interactions in the surface of the coating and also by the addition of polysaccharides and lipids. It was obtained values under and above 90^{o}. However, most of the samples showed angles between 70^{o} and 90^{o} referring hydrophilicity which is beneful for stem cell attachment and cell migration. Rheology revealed that 10% PCL had better storage values (elastic part) and that xanthan gum gives stability and stiffness to PCL. Loss modulus indicated stability in composte membranes causing less dissipated energy. The material presented non-Newtonial behavior having big slopes in its viscosity values (shear thinning), while damping factor showed an hyper-elastic

behavior due to strong interaction between the polymer chains, causing less internal frictions. In summary, a new intelligent synthetic material has been developed for surgical meshes in the repair of abdominal wall hernias, which, through chemical modifications and the use of solvents such as dimethylformamide and chloroform obtained an ideal porosity for cell migration and proliferation in both parts of the coating, allowing this characteristic, since the diameter of a stem cell is between 15 and 30 μm. Likewise, the incorporation of biocomponents such as hyaluronic acid, vitamin E, polylysine, among others, provide excellent cellular compatibility by allowing migration, proliferation, and growth, also promoting anti-inflammatory behavior and anti-adhesive properties. In addition, the use of xanthan gum, propylene glycol, vitamin E, and hyaluornic acid provide differentiated viscoelastic and mechanical properties because these materials have crosslinking properties and some of them act as plasticizers that improve mechanical behavior, allowing to resist different body mechanisms as peristaltic movements. Through the use of stem cells, tissue regeneration will be improved since these cells have the characteristic of being able to differentiate into different types of cells such as myocytes, adipocytes, and chondrocytes, which allow tissue regeneration, in addition to possessing biological properties that improve the synthesis of collagen and fibrin which helps in the wound healing process, as well as the promotion of vascular growth factors, fibroblasts and modulate anti-inflammatory cytokines such as IL4, IL-10, TNF-B. Together, the three mechanisms will provide the necessary conditions to reduce the post-operative immune response, such as infections, recurrences, having a controlled inflammatory response, favoring wound repair, and improving incorporation with the body. Therefore, the development of an intelligent synthetic coating was possible with superior characteristics than commercial meshes, and with significant advances in the state of the art, which will give the possibility of preserving abdominal wall integrity to patients suffering from this problem.

5.0.1 Contributions

1. A novel prototype of intelligent synthetic coating material with the use of biomaterials such as PCL, hyaluronic acid and vitamin E.

2. A new method to modify polymer structure having changes in morphology, wettability and hyper elastic behavior by the inclusion of chemical process and solvents.

3. A novel material capable of promote wound healing and regeneration of tissue by the use of stem cell therapy.

4. A new contribution to the state of the art since the behavior of a coating of hyaluronic

acid, vitamin E and polycaprolactone in conjunction with stem cells has not been studied.

5.0.2 Future Work

1. Characterize the mechanical properties in order to evaluate mechanical behavior and comparing with human body conditions.

2. Characterize the bio-mechanical properties with degradation tests and post-implantation analysis, evaluating loss of mechanical properties as tensile strength, stiffness, breaking strength, etc.

3. Improve biological properties by the use of adipose stem cells will be integrated into the mesh.

4. Perform a stem cell culture to be used in the coating.

5. Evaluate the biological behavior of stem cells with studies such as cell growth, cell viability, cell differentiation and cell proliferation will be performed.

6. Study the in-vivo response of the coating with stem cells, thus, animal models are needed. Will be performed assays of cytotoxicity, biocompatibility, ECM components and histology analysis.

Appendix A

Appendix

Your appendix should go here.

Bibliography

[1] Karen Baylon, Perla Rodr, Alex El, Jose Antonio D, Robert Gilkerson, and Karen Lozano. Past , Present and Future of Surgical Meshes : A Review. *Membranes*, pages 1–23, 2017.

[2] R. Bittner and J. Schwarz. Inguinal hernia repair: Current surgical techniques. *Langenbeck's Archives of Surgery*, 397(2):271–282, 2012.

[3] John T Jenkins and Patrick J O'Dwyer. Inguinal hernias. *Bmj*, 336(7638):269–272, 2008.

[4] Kathleen Lockhart, Edward Teo, Shawn Teo, Manvinder Dhillon, and Mieke L. van Driel. Mesh versus non-mesh for inguinal and femoral hernia repair. *Cochrane Database of Systematic Reviews*, 2015(2), 2015.

[5] C. N. Brown and J. G. Finch. Which mesh for hernia repair?, 2010.

[6] Mike Driver. Preface. In Mike Driver, editor, *Coatings for Biomedical Applications*, Woodhead Publishing Series in Biomaterials, pages xiii – xiv. Woodhead Publishing, 2012.

[7] A. H. Petter-Puchner, R. H. Fortelny, S. Gruber-Blum, H. Redl, and U. Dietz. The future of stem cell therapy in hernia and abdominal wall repair. *Hernia*, 19(1):25–31, 2015.

[8] Thomas V Johnson and Keith R Martin. *Stem Cells: A Future Glaucoma Therapy?* Elsevier Ltd, second edi edition.

[9] Chris Mason and Peter Dunnill. A brief definition of regenerative medicine. 3:1–5, 2008.

[10] Surge Kalaba, Ethan Gerhard, Joshua S Winder, Eric M Pauli, and Randy S Haluck. Design strategies and applications of biomaterials and devices for Hernia repair. *Bioactive Materials*, 1(1):2–17, 2016.

[11] Tianzhu Zhang, Zhigang Zhang, Wanjun Hu, Zhenling Ji, and Ning Gu. Preparation of poly(vinyl alcohol) modified polypropylene mesh and its antiadhesion efficacy in experimental hernia repair. *Colloids and Surfaces A: Physicochemical and Engineering Aspects*, 500:10–16, 2016.

[12] L. Liu, C. Petro, A. Majumder, M. Fayezizadeh, J. Anderson, and Y. W. Novitsky. The use of Vicryl mesh in a porcine model to assess its safety as an adjunct to posterior fascial closure during retromuscular mesh placement. *Hernia*, 20(2):289–295, 2016.

[13] Omaima Tawfiq Alomani, Sheema Mohammed Alqhtani, Shuroq Abdulmohsen Alshehri, and Omar Hatem Taha. Advantages and Efficiency of Immediate Vicryl Mesh Insertion after Lumpectomy. 5(2):250–255, 2018.

[14] Robert Bendavid. Abdominal wall hernias principles and management, 2001.

[15] Ali Rastegarpour, Michael Cheung, Madhurima Vardhan Ms, Mohamed M Ibrahim, Charles E Butler Facs, Howard Levinson, A Rastegarpour, M Cheung, M Vardhan, and M M Ibrahim. Surgical mesh for ventral incisional hernia repairs : Understanding mesh design. 24(1):41–50, 2016.

[16] Bernd Klosterhalfen. The lightweight and large porous mesh concept for hernia repair. (June 2014), 2005.

[17] Brentley A Buchele, Siroos S Shirazi, and Lyle B Hunt. Use of an Absorbable Mesh to Repair Contaminated Abdominal-Wall Defects. 52242, 2015.

[18] Olivier Guillaume, Andreas Herbert Teuschl, Simone Gruber-blum, René Hartmann Fortelny, Heinz Redl, and Alexander Petter-puchner. Emerging Trends in Abdominal Wall Reinforcement : Bringing Bio-Functionality to Meshes. pages 1763–1789, 2015.

[19] Arthur P Fine. Laparoscopic repair of inguinal hernia using Surgisis mesh and fibrin sealant. *JSLS : Journal of the Society of Laparoendoscopic Surgeons / Society of Laparoendoscopic Surgeons*, 10(4):461–5, 2006.

[20] Mike Ralf and Langenbach Æ Johannes. Sixty-month follow-up after endoscopic inguinal hernia repair with three types of mesh : a prospective randomized trial. pages 1790–1797, 2008.

[21] a I Gilbert, M F Graham, and W J Voigt. A complication of the use of Prolene mesh in the repair of abdominal wall hernias. *Hernia*, 2:161–166, 1998.

[22] H S Goldstein. Selecting the right mesh. pages 23–26, 1999.

[23] Rita Rynkevic, Pedro Martins, António A Fernandes, and Francisco Pereira. In vitro study of the mechanical performance of hernia mesh under cyclic loading. *Journal of Materials Science: Materials in Medicine*, pages 1–7, 2017.

[24] Thomas Kolbe, Æ Christian Hollinsky, Ingrid Walter, Æ Anja Joachim, and Æ Thomas Ru. Influence of a new self-gripping hernia mesh on male fertility in a rat model Influence of a new self-gripping hernia mesh on male fertility in a rat model. (August), 2009.

[25] Peter P Pott, Markus L R Schwarz, Ralf Gundling, Kai Nowak, Peter Hohenberger, and Eric D Roessner. Mechanical Properties of Mesh Materials Used for Hernia Repair and Soft Tissue Augmentation. 7(10):1–10, 2012.

[26] Bartira M Soares, Robert G Guidoin, Yves Marois, Louisette Martin, Martin W King, Gaktan Laroche, Ze Zhang, Jamal Charara, and Jean-franqois Girard. In vivo characterization of a fluoropassivated gelatin- impregnated polyester mesh for hernia repair. 32:293–305, 1996.

[27] Gerhard Rakhorst and Rutger Ploeg. *Biomaterials in Modern Medicine: The Groningen Perspective*. 2008.

[28] Anton F Engelsman, Henny C Van Der Mei, Rutger J Ploeg, and Henk J Busscher. The phenomenon of infection with abdominal wall reconstruction. 28:2314–2327, 2007.

[29] H G Doctor. Evaluation of various prosthetic materials and newer meshes for hernia repairs. 2(3):110–116, 2006.

[30] Richard H Koehler, Dennis Begos, Dieter Berger, Steve Carey, Karl Leblanc, Adrian Park, Bruce Ramshaw, Roy Smoot, and Guy Voeller. Minimal Adhesions to ePTFE Mesh After Laparoscopic Ventral Incisional Hernia Repair : Reoperative Findings in 65 Cases. (April 1993):335–340, 2003.

[31] Roger K J Simmermacher, Robert P Bleichrodt, and Jeff M Schakenraad. Review : Biomaterials for Abdominal Wall Reconstruction. 2(4), 1992.

[32] Santhini Elango, Sakthivel Perumalsamy, Krishnakumar Ramachandran B Tech, and Ketankumar Vadodaria. Mesh materials and hernia repair. 7(3):14–23, 2017.

[33] Sean B Orenstein, Ean R Saberski, Donald L Kreutzer, D Ph, and Yuri W Novitsky. Comparative Analysis of Histopathologic Effects of Synthetic Meshes Based on Material , Weight , and Pore Size in Mice. *Journal of Surgical Research*, 176(2):423–429, 2012.

[34] Lei-ming Zhu, Philipp Schuster, and Uwe Klinge. Mesh implants : An overview of crucial mesh parameters. 7(10):226–236, 2015.

[35] Thomas Goedderz Thomas Muhl, Marcel Binnebosel, Uwe Klinge. New Objective Measurement to Characterize the Porosity of Textile Implants. *Journal of biomedical materials research. Part B, Applied biomaterials*, 82(1):174–182, 2007.

[36] Farzad Kakaei, Mir Salim, Seyyed Sadeghi, Behnam Sanei, Shahryar Hashemzadeh, and Afshin Habibzadeh. A Randomized Clinical Trial Comparing the Effect of Different Haemostatic Agents for Haemostasis of the Liver after Hepatic Resection. 2013, 2013.

[37] Ph Topart, Æ L Ferrand Æ F Vandenbroucke, and Æ P Lozac. Laparoscopic ventral hernia repair with the Goretex Dualmesh : long-term results and review of the literature. pages 348–352, 2005.

[38] J M Bellh, J Bujh, L A Contreras, A Cameras-san Martin, A Hernando, and F Jurado. Improvement of the tissue integration of a new modified polytetrafluoroethylene prosthesis : Mycro Mesh @. 17(13):1265–1271, 1996.

[39] J M Bellon, L A Contreras, C Campo, and A Hernando. A new type of polytetrafluoroethylene prosthesis (Mycro Mesh): an experimental study. 7:475–478, 1996.

[40] J Rouet, G Bwelle, F Cauchy, and P Masso-misse. Polyester mosquito net mesh for inguinal hernia repair : A feasible option in resource limited settings in Cameroon ? *Journal of Visceral Surgery*, 2017.

[41] Noor Sanbhal, Ying Mao, Gang Sun, Yan Li, Mazhar Peerzada, and Lu Wang. Preparation and Characterization of Antibacterial Polypropylene Meshes with Covalently Incorporated β -Cyclodextrins and Captured Antimicrobial Agent for Hernia Repair. 2018.

[42] Umran Aydemir Sezer, Vildan Sanko, Mehmet Gulmez, Elif Sayman, Basak Aru, Zehra Nur Yuksekdag, Ali Aktekin, Fugen Vardar Aker, and Serdar Sezer. A Polypropylene-Integrated Bilayer Composite Mesh with Bactericidal and Antiadhesive Efficiency for Hernia Operations. *ACS Biomaterials Science and Engineering*, 3(12):3662–3674, 2017.

[43] Kristóf; Molnár, Constantinos; Voniatis, Daniella; Fehér, Andrea; Ferencz, László; Fónyad, Lilla; Reiniger, Miklós; Zrínyi, György; Wéber, and Angela; Jedlovszky-hajdu. Biocompatibility study of poly(vinyl alcohol) based electrospun scaffold for hernia repair. *Express Polymer Letters*, 12(8):676–687, 2018.

[44] Krisztina Juhos, Péter Szentes, Domokos Csukás, and József Sándor. ABDOMINAL HERNIA REPAIR WITH POLY(SUCCINIMIDE) AND WITH ITS CYSTEAMINE CROSSLINKED NANOFIBER HERNIA MESHES. A PRELIMINARY EXPERIMENTAL STUDY. 6(2):1–6, 2016.

[45] Jeffrey A Blatnik, Thimma R Thatiparti, David M Krpata, Sean T Zuckerman, Michael J Rosen, and Horst A Von Recum. Infection prevention using affinity polymer-coated , synthetic meshes in a pig hernia model. *Journal of Surgical Research*, 219:5–10, 2017.

[46] J. R. Eriksen, I. Gögenur, and J. Rosenberg. Choice of mesh for laparoscopic ventral hernia repair. *Hernia*, 11(6):481–492, 2007.

[47] Jaro Rosenberg and J. Burcharth. Feasibility and outcome after laparoscopic ventral hernia repair using Proceed mesh. *Hernia*, 12(5):453–456, 2008.

[48] B. P. Jacob, N. J. Hogle, E. Durak, T. Kim, and D. L. Fowler. Tissue ingrowth and bowel adhesion formation in an animal comparative study: Polypropylene versus Proceed versus Parietex Composite. *Surgical Endoscopy and Other Interventional Techniques*, 21(4):629–633, 2007.

[49] Parag Bhanot, Brenton R. Franklin, and Ketan M. Patel. Proceed^{TM} Mesh for Laparoscopic Ventral Hernia Repair. *JSLS : Journal of the Society of Laparoendoscopic Surgeons*, 17(4):565–569, 2014.

[50] Timothy W. Judge, David M. Parker, and Robert C. Dinsmore. Abdominal Wall Hernia Repair: A Comparison of Sepramesh and Parietex Composite Mesh in a Rabbit Hernia Model. *Journal of the American College of Surgeons*, 204(2):276–281, 2007.

[51] F. Köckerling and C. Schug-Pass. What do we know about titanized polypropylene meshes? An evidence-based review of the literature. *Hernia*, 18(4):445–457, 2014.

[52] Maria de Lourdes Pessole ; Victor Cezar de azevedo Pessini ; Pedro Henrique Caldeira Porto Biondo-simões and Robes ; Rogério Ribeiro. Adhesions on polypropylene versus Sepramesh® meshes: an experimental study in rats. 45(6):1–11, 1996.

[53] Keith E. Greenawalt, Timothy J. Butler, Eric A. Rowe, Amy C. Finneral, David S. Garlick, and James W. Burns. Evaluation of sepramesh biosurgical composite in a rabbit hernia repair model. *Journal of Surgical Research*, 94(2):92–98, 2000.

[54] Nelleke Schouten, Thijs van Dalen, Niels Smakman, Sjoerd G. Elias, Geert J. Clevers, Egbert Jan M.M. Verleisdonk, Paul H.P. Davids, and Ine P.J. Burgmans. The effect of ultrapro or prolene mesh on postoperative pain and well-being following endoscopic Totally Extraperitoneal (TEP) hernia repair (TULP): Study protocol for a randomized controlled trial. *Trials*, 13(1):1, 2012.

[55] Robert J. Fitzgibbons Volker Schumpelick. *Hernia Repair Sequelae*. Springer-Verlag Berlin Heidelberg New York, 2010.

[56] U. Klinge and B. Klosterhalfen. Modified classiffication of surgical meshes for hernia repair based on the analyses of 1,000 explanted meshes. *Hernia*, 16(3):251–258, 2012.

[57] Filip Muysoms, Roel Beckers, and Iris Kyle-Leinhase. Prospective cohort study on mesh shrinkage measured with MRI after laparoscopic ventral hernia repair with an intraperitoneal iron oxide-loaded PVDF mesh. *Surgical Endoscopy*, 32(6):2822–2830, 2018.

[58] Samir Delibegovic, Anhel Koluh, Elmir Cickusic, Muhamed Katica, Jasminka Mustedanagic, and Ferid Krupic. Formation of adhesion after intraperitoneal application of TiMesh: Experimental study on a rodent model. *Acta Chirurgica Belgica*, 116(5):293–300, 2016.

[59] Verónica Gómez-Gil, Marta Rodríguez, Francisca García-Moreno Nisa, Bárbara Pérez-Köhler, and Gemma Pascual. Evaluation of synthetic reticular hybrid meshes designed for intraperitoneal abdominal wall repair: Preclinical and in vitro behavior. *PLoS ONE*, 14(2):1–26, 2019.

[60] Christine Schug-Pass, Florian Sommerer, Andrea Tannapfel, Hans Lippert, and Ferdinand Köckerling. Does the additional application of a polylactide film (surgiwrap) to a lightweight mesh (timesh) reduce adhesions after laparoscopic intraperitoneal implantation procedures? experimental results obtained with the laparoscopic porcine model. *Surgical Endoscopy*, 22:2433–2439, 2008.

[61] Christine Schug-Pass, Claudia Tamme, Andrea Tannapfel, and Ferdinand Köckerling. A lightweight polypropylene mesh (timesh) for laparoscopic intraperitoneal repair of abdominal wall hernias. *Surgical Endoscopy And Other Interventional Techniques*, 20:402–409, 2004.

[62] Raphael Rosch, K. Junge, R. Quester, U. Klinge, B. Klosterhalfen, and V. Schumpelick. Vypro II® mesh in hernia repair: Impact of polyglactin on long-term incorporation in rats. *European Surgical Research*, 35(5):445–450, 2003.

[63] Mingtai Gao, Jianxu Han, Jinhui Tian, and Kehu Yang. Vypro II Mesh for Inguinal Hernia Repair. *Annals of Surgery*, 251(5):838–842, 2010.

[64] Sven Bringman, Timo Jaakko Heikkinen, Staffan Wollert, Johanna Österberg, Sam Smedberg, Håkan Granlund, Stig Ramel, Göran Felländer, and Bo Anderberg. Early results of a single-blinded, randomized, controlled, internet-based multicenter trial comparing Prolene and Vypro II mesh in Lichtenstein hernioplasty. *Hernia*, 8(2):127–134, 2004.

[65] Yilmaz Bilsel and Ilker Abci. The search for ideal hernia repair ; mesh materials and types. *International Journal of Surgery*, 10(6):317–321, 2012.

[66] Andrew N. Kingsnorth ; Karl A. LeBlanc. *Management of Abdominal Hernias*. Springer-Verlag London, 4 edition, 2013.

[67] V Amar, F N B Mas, G Premalatha, K B Gayathri, and P R K Bhargav. Recurrent Incisional Hernia After Laparoscopic Parietex Mesh Repair. pages 1–4.

[68] F Jurczak and H Khalil. First Year Preliminary Results on the Use of a Monofilament Polyester Mesh With a Collagen Barrier for Primary and Incisional Ventral. pages 56–65, 2018.

[69] Aali J Sheen, J James Pilkington, Minas Baltatzis, Ahmed Tyurkylmaz, Panagiotis Stathakis, Saurabh Jamdar, and Ajith K Siriwardena. Comparison of Mesh Fixation Techniques in Elective Laparoscopic Repair of Incisional Hernia-ReliaTack ™ v Pro-Tack ™ (TACKoMesh) - A double-blind randomised controlled trial. pages 1–7, 2018.

[70] Amir Ben, Yehuda Abraham, and Nyska Amir. Mesh fixation using novel bio - adhesive coating compared to tack fixation for IPOM hernia repair : in vivo evaluation in a porcine model. *Surgical Endoscopy*, (0123456789), 2019.

[71] J Brand, R H Fortelny, N Walder, W Oehlinger, F Koenig, and H Redl. Comparison of three separate antiadhesive barriers for intraperitoneal onlay mesh hernia repair in an experimental model. pages 442–449, 2011.

[72] Corey R Deeken and Brent D Matthews. Ventralight ST and SorbaFix Versus Physiomesh and Securestrap in a Porcine Model. pages 549–559, 2013.

[73] Surgical Technology, International Xxvi, Epartment Of, Epartment Of, Epartment Of, Epartment Of, and Epartment Of. Long-term Outcome on the use of the Ventralight ™ ST Hernia Patch in ABSTRACT. (July 2011), 2013.

[74] E. Vailhe. Mesh competitor testing,(AST-2015-0024, performance evaluation technical report). Technical report, 2015.

[75] Karsten Junge, R. Rosch, U. Klinge, M. Saklak, B. Klosterhalfen, C. Peiper, and V. Schumpelick. Titanium coating of a polypropylene mesh for hernia repair: Effect on biocompatibilty. *Hernia*, 9(2):115–119, 2005.

[76] Hrishikesh Salgaonkar and Davide Lomanto. Mesh technology — an update. pages 1–10, 2018.

[77] Kevin El-hayek, Cleveland Clinic, Abu Dhabi, and Bipan Chand. Biologic Prosthetic Materials for Hernia Repairs. (May), 2014.

[78] Yuri W Novitsky. *Hernia Surgery*.

[79] Ciara R Huntington, Tiffany C Cox, Laurel J Blair, Samuel Schell, David Randolph, Tanushree Prasad, and Amy Lincourt. Biologic mesh in ventral hernia repair : Outcomes , recurrence , and charge analysis. *Surgery*, pages 1–11, 2016.

[80] Daniel Albo, D Ph, Samir S Awad, David H Berger, and Charles F Bellows. Decellularized human cadaveric dermis provides a safe alternative for primary inguinal hernia repair in contaminated surgical fields. 192:12–17, 2006.

[81] David M Parker, Peter J Armstrong, and John W Tsai. Comparison of Surgisis Ò , AlloDerm Ò , and Vicryl Woven Mesh Ò Grafts for Abdominal Wall Defect Repair in an Animal Model. pages 290–296, 2010.

[82] Jin Yoo. Mesh Selection for Open and Laparoscopic Hernia Repair, 2019.

[83] Justin M Broyles, Nicholas B Abt, Justin M Sacks, and Charles E Butler. Bioprosthetic Tissue Matrices in Complex. pages 1–7.

[84] Michael J Rosen. *Atlas of Abdominal Wall Reconstruction Library of Congress Cataloging-in-Publication Data*.

[85] Kathryn S King and Frank P Albino. Biologic mesh for abdominal wall reconstruction. pages 57–65, 2014.

[86] Steven T. Brower Cohn, Stephen M. Cohn. *Surgery: evidence-based practice*. PMPH-USA, illustrate edition, 2012.

[87] V. Lambropoulos, E. Mylona, V. Mouravas, C. Tsakalidis, I. Spyridakis, G. Mitsiakos, and P. Karagianni. Repair of Postoperative Abdominal Hernia in a Child with Congenital Omphalocele Using Porcine Dermal Matrix. *Case Reports in Medicine*, 2016:1–5, 2016.

[88] Frank E Primus and Hobart W Harris. A Critical Review of Biologic Mesh Use in Ventral Hernia Repairs under Contaminated Conditions. 17(1):21–30, 2014.

[89] F. Köckerling, N. N. Alam, S. A. Antoniou, I. R. Daniels, F. Famiglietti, R. H. Fortelny, M. M. Heiss, F. Kallinowski, I. Kyle-Leinhase, F. Mayer, M. Miserez, A. Montgomery, S. Morales-Conde, F. Muysoms, S. K. Narang, A. Petter-Puchner, W. Reinpold, H. Scheuerlein, M. Smietanski, B. Stechemesser, C. Strey, G. Woeste, and N. J. Smart. What is the evidence for the use of biologic or biosynthetic meshes in abdominal wall reconstruction? *Hernia*, 22(2):249–269, 2018.

[90] Ethicon. FlexHD Acellular Hydrated Dermis for Breast Reconstruction, 2019.

[91] Angela Cheng and Michel Saint-Cyr. Comparison of Different ADM Materials in Breast Surgery. *Clinics in Plastic Surgery*, 39(2):167–175, 2012.

[92] Manh Dan Ngo, Harold M. Aberman, Michael L. Hawes, Bryan Choi, and Arthur A. Gertzman. Evaluation of human acellular dermis versus porcine acellular dermis in an in vivo model for incisional hernia repair. *Cell and Tissue Banking*, 12(2):135–145, 2011.

[93] F. Catena, L. Ansaloni, A. Leone, A. De Cataldis, S. Gagliardi, F. Gazzotti, S. Peruzzi, S. Agrusti, L. D'Alessandro, and M. Taffurelli. Lichtenstein repair of inguinal hernia with Surgisis inguinal hernia matrix soft-tissue graft in immunodepressed patients. *Hernia*, 9(1):29–31, 2005.

[94] Sara Armitage, Elvis I. Seman, and Marc J. N. C. Keirse. Use of Surgisis for Treatment of Anterior and Posterior Vaginal Prolapse. *Obstetrics and Gynecology International*, 2012:1–5, 2012.

[95] Jeffrey C Y Chan, Krishna Burugapalli, Yi-shiang Huang, John L Kelly, Abhay Pandit, Biomedical Engineering Theme, United Kingdom, Jeffrey Chee, Yean Chan, and Krishna Burugapalli. Cross-linked cholecyst-derived extracellular matrix for abdominal wall repair. pages 1–45, 2017.

[96] Andrey Nikolayevich ZharikovV.G. LubyanskyE.K. Gladysheva. Prosthetic hernioplasty using bacterial nanocellulose: an experimental study. pages 59–66, 2018.

[97] Arvind U Gowda, Colton H L Mcnichols, Ishan Asokan, Jamil A Matthews, E Bryan Buckingham, Jennifer Sabino, John S Maddox, Sheri Slezak, Yvonne Rasko, and P Devinder. Porcine Acellular Dermal Matrix for Hernia Repair in Transplant Patients. 77(6), 2016.

[98] Cook Biotech. Cook Introduces Zenapro™ Hybrid Hernia Repair Device, 2014.

[99] Spencer P. Lake, Nathaniel F.N. Stoikes, Amit Badhwar, and Corey R. Deeken. Contamination of hybrid hernia meshes compared to bioresorbable Phasix™ Mesh in a rabbit subcutaneous implant inoculation model. *Annals of Medicine and Surgery*, 46(May):12–16, 2019.

[100] Mangala Joshi and Bapan Adak. *Advances in Nanotechnology Based Functional, Smart and Intelligent Textiles: A Review*. Elsevier Ltd., 2019.

[101] B Yelimlies Æ A Alponat Æ A C and Æ C Erc. Carboxymethylcellulose coated on visceral face of polypropylene mesh prevents adhesion without impairing wound healing in incisional hernia model in rats. pages 130–133, 2003.

[102] S. Kyzer, A. Kadouri, A. Levi, E. Ramadan, H. Levinsky, M. Halpern, and C. Chaimoff. Repair of fascia with polyglycolic acid mesh cultured with fibroblasts – experimental study. *European Surgical Research*, 29(2):84–92, 1997.

[103] M. Van't Riet, J. W.A. Burger, F. Bonthuis, J. Jeekel, and H. J. Bonjer. Prevention of adhesion formation to polypropylene mesh by collagen coating: A randomized controlled study in a rat model of ventral hernia repair. *Surgical Endoscopy and Other Interventional Techniques*, 18(4):681–685, 2004.

[104] U. Klinge, B. Klosterhalfen, M. Müller, M. Anurov, A. Öttinger, and V. Schumpelick. Influence of polyglactin-coating on functional and morphological parameters of polypropylene-mesh modifications for abdominal wall repair. *Biomaterials*, 20(7):613–623, 1999.

[105] Karla Lehle, Stefan Lohn, Günter Reinerth, Thomas Schubert, Jürgen G. Preuner, and Dietrich E. Birnbaum. Cytological evaluation of the tissue-implant reaction associated with subcutaneous implantation of polymers coated with titaniumcarboxonitride in vivo. *Biomaterials*, 25(24):5457–5466, 2004.

[106] H. Scheidbach, A. Tannapfel, U. Schmidt, H. Lippert, and F. Köckerling. Influence of titanium coating on the biocompatibility of a heavyweight polypropylene mesh an animal experimental model. *European Surgical Research*, 36(5):313–317, 2004.

[107] J. Zhao and J. J. Xu. Experimental study on application of polypropylene hernia of fat stem cells in rats. *European Review for Medical and Pharmacological Sciences*, 22(18):6156–6161, 2018.

[108] A. N. Baird Dean A. Hendrickson. *Turner and McIlwraith's Techniques in Large Animal Surgery*. Wiley-Blackwell, 4 edition, 2013.

[109] Daniela Hutanu. Recent Applications of Polyethylene Glycols (PEGs) and PEG Derivatives. *Modern Chemistry & Applications*, 02(02):2–7, 2014.

[110] Rimpro India. Polyethylene Glycol, 2019.

[111] H. Scheuerlein, J. Erdmann, F. Rauchfuss, Y. Dittmar, K. Jandt, K. Jandt, U. Settmacher, and S. Zankovych. Herstellung und In-vitro-Analyse einer Polyethylenimin-Beschichtung auf Herniennetzen. *Zentralblatt für Chirurgie - Zeitschrift für Allgemeine, Viszeral-, Thorax- und Gefäßchirurgie*, 140(02):170–178, 2015.

[112] Zheng Zhang, Ophir Ortiz, Ritu Goyal, and Joachim Kohn. *Biodegradable Polymers*. Elsevier, fourth edi edition, 2014.

[113] Oral Saygun, Canan Agalar, Kuzey Aydinuraz, Fatih Agalar, Cagatay Daphan, Meral Saygun, Sabahat Ceken, Abdullah Akkus, and Emir Baki Denkbas. Gold and gold-palladium coated polypropylene grafts in a S. epidermidis wound infection model. *Journal of Surgical Research*, 131(1):73–79, 2006.

[114] Alice F Versiani, Lídia M Andrade, Estefânia M N Martins, Sérgio Scalzo, Jony M Geraldo, Claudilene R Chaves, Daniele C Ferreira, Marina Ladeira, Silvia Guatimosim, Luiz O Ladeira, and Flávio G Fonseca. Gold nanoparticles and their applications in biomedicine. 2016.

[115] M. Kapischke, K. Prinz, J. Tepel, J. Tensfeldt, and T. Schulz. Precoating of alloplastic materials with living human fibroblasts: A feasibility study. *Surgical Endoscopy and Other Interventional Techniques*, 19(6):791–797, 2005.

[116] I R Fernandes, F B Russo, G C Pignatari, M M Evangelinellis, S Tavolari, A R Muotri, and P C B Beltra. Fibroblast sources : Where can we get them ? pages 223–228, 2016.

[117] U. Klueh, V. Wagner, S. Kelly, A. Johnson, and J. D. Bryers. Efficacy of silver-coated fabric to prevent bacterial colonization and subsequent device-based biofilm formation. *Journal of Biomedical Materials Research*, 53(6):621–631, 2000.

[118] Khalid Alaqad and Tawfik A Saleh. Gold and Silver Nanoparticles: Synthesis Methods, Characterization Routes and Applications towards Drugs. *Journal of Environmental & Analytical Toxicology*, 6(4), 2016.

[119] Giuliana Muzio, Sergio Perero, Marta Miola, Manuela Oraldi, Sara Ferraris, Enrica Verne, Federico Festa, Rosa Angela Canuto, Valentino Festa, and Monica Ferraris. Biocompatibility versus peritoneal mesothelial cells of polypropylene prostheses for hernia repair , coated with a thin silica / silver layer. pages 1–8, 2016.

[120] Anna England, Ana M. Valdes, Joanne L. Slater-Jefferies, Rosalynn Gill, W. Martin Howell, Philip C. Calder, and Robert F. Grimble. Variants in the genes encoding TNF-α, IL-10, and GSTP1 influence the effect of α-tocopherol on inflammatory cell responses in healthy men. *American Journal of Clinical Nutrition*, 95(6):1461–1467, 2012.

[121] M. A. Keen and I. Hassan. Vitamin e in dermatology. *Indian Dermatol Online*, pages 311–315, 2016.

[122] Dmitry Gil, James Rex, William Cobb, Vladimir Reukov, and Alexey Vertegel. Anti-inflammatory coatings of hernia repair meshes: A pilot study. *Journal of Biomedical Materials Research - Part B Applied Biomaterials*, 106(2):589–597, 2018.

[123] Gore. What is ePTFE?, 2015.

[124] N Deligiannidis Æ I Papavasiliou Æ K Sapalidis and I Kesisoglou Æ S Papavramidis Æ O Gamvros. The use of three different mesh materials in the treatment of abdominal wall defects. pages 51–55, 2002.

[125] Marc H.F. Schreinemacher, Kevin W.Y. Van Barneveld, Rieky E.G. Dikmans, Marion J.J. Gijbels, Jan Willem M. Greve, and Nicole D. Bouvy. Coated meshes for hernia

repair provide comparable intraperitoneal adhesion prevention. *Surgical Endoscopy*, 27(11):4202–4209, 2013.

[126] Natasha Udpa, Shama R. Iyer, Rohit Rajoria, Kate E. Breyer, Helen Valentine, Bhupinder Singh, Sean P. McDonough, Bryan N. Brown, Lawrence J. Bonassar, and Yingxin Gao. Effects of chitosan coatings on polypropylene mesh for implantation in a rat abdominal wall model. *Tissue Engineering - Part A*, 19(23-24):2713–2723, 2013.

[127] Andrew Bates S. Scott Davis, Jr., Gregory Dakin. *The SAGES Manual of Hernia Surgery*. Springer, 2 edition, 2018.

[128] James M Massullo, Tejinder P Singh, Ward J Dunnican, and Brian R Binetti. Preliminary Study of Hiatal Hernia Repair Using Polyglycolic Acid : Trimethylene Carbonate Mesh. pages 55–59, 2012.

[129] Jochen Reinbold, Teresa Hierlemann, Lukas Urich, Ann Kristin Uhde, Ingrid Müller, Tobias Weindl, Ulrich Vogel, Christian Schlensak, Hans Peter Wendel, and Stefanie Krajewski. Biodegradable rifampicin-releasing coating of surgical meshes for the prevention of bacterial infections. *Drug Design, Development and Therapy*, 11:2753–2762, 2017.

[130] James F Fitzgerald and Anjali S Kumar. Biologic versus Synthetic Mesh Reinforcement : What are the Pros and Cons ? pages 140–148, 2014.

[131] C. C. Chu and L. Welch. Characterization of morphologic and mechanical properties of surgical mesh fabrics. *Journal of Biomedical Materials Research*, 1985.

[132] J. Li, Z. Ji, and T. Cheng. Lightweight versus heavyweight in inguinal hernia repair: A meta-analysis. *Hernia*, 16(5):529–539, 2012.

[133] A. Coda, R. Lamberti, and S. Martorana. Classification of prosthetics used in hernia repair based on weight and biomaterial. *Hernia*, 16(1):9–20, 2012.

[134] David B. Earle and Lisa A. Mark. Prosthetic Material in Inguinal Hernia Repair: How Do I Choose? *Surgical Clinics of North America*, 88(1):179–201, 2008.

[135] Hongyi Liu, Weibin Chen, Bin Zhao, Wei Quan, Yinlong Zhang, Yuanyuan Zhou, Zheng Wan, Xiaohong Zhang, Gang Xue, Jietao Li, Shuting Luo, Jinling Wang, Yun Liu, Maochuan Zhen, and Yilin Zhao. Autologous bionic tissue for inguinal hernia repair. *Journal of Biomedical Materials Research - Part A*, 2020.

[136] S. Todros, P. G. Pavan, and A. N. Natali. Biomechanical properties of synthetic surgical meshes for pelvic prolapse repair. *Journal of the Mechanical Behavior of Biomedical Materials*, 55:271–285, 2016.

[137] Derek A. DuBay, Xue Wang, Belinda Adamson, William M. Kuzon, Robert G. Dennis, and Michael G. Franz. Mesh incisional herniorrhaphy increases abdominal wall elastic properties: A mechanism for decreased hernia recurrences in comparison with suture repair. *Surgery*, 140(1):14–24, 2006.

[138] Guilherme Barreiro, Vinícius S. de Lima, and Leandro T. Cavazzola. Abdominal skin tensile strength in aesthetic and massive weight loss patients and its role in ventral hernia repair. *BMC surgery*, 19(1):68, 2019.

[139] Corey R Deeken and Spencer P Lake. Mechanical Properties of the Abdominal Wall and Biomaterials Utilized for Hernia Repair. *Journal of the Mechanical Behavior of Biomedical Materials*, 2017.

[140] Giboni M Niewiera. Elasticity of the anterior abdominal wall and impact for reparation of incisional hernias using mesh implants. pages 113–118, 2001.

[141] Noor Sanbhal, Linli Miao, Rui Xu, Awais Khatri, and Lu Wang. Physical structure and mechanical properties of knitted hernia mesh materials : A review. 2018.

[142] Ahmed M S Ibrahim, Christina R Vargas, Samuel J Lin, and Bernard T Lee. Properties of Meshes used in Hernia Repair : A Comprehensive Review of Synthetic and Biologic Meshes. 1(212), 2015.

[143] Braden J Eliason, Margaret M Frisella, Brent D Matthews, and Corey R Deeken. Effect of Repetitive Loading on the Mechanical Properties of Synthetic Hernia Repair Materials. *ACS*, 213(3):430–435, 2011.

[144] Biologische Matrizes and Rahmen Der. Biological Matrices and Synthetic Meshes Used in Implant-based Breast Reconstruction – a Review of Products Available in Germany. pages 1100–1106.

[145] Bard. XenMatrix surgical graft, 2019.

[146] Baxter. Veritas collagen matrix, 2019.

[147] Sachin Mane. Effect of Porogens (Type and Amount) on Polymer Porosity : A Review. 4(2):210–225, 2016.

[148] Sachin Mane, Surendra Ponrathnam, and Nayaku Chavan. Role of Interfacial Tension of Solvating Diluents and Hydrophilic Hydrophobic Cross-Linkers in Hyper-Cross-Linked Solid Supports. 2015.

[149] Mohamed H. Mohamed and Lee D. Wilson. Porous Copolymer Resins: Tuning Pore Structure and Surface Area with Non Reactive Porogens. *Nanomaterials*, 2(2):163–186, 2012.

[150] Yuanbo Cai, Wu Yan, Xuesong Peng, Mei Liang, Lin Yu, and Huawei Zou. Influence of solubility parameter difference between monomer and porogen on structures of poly (acrylonitrile–styrene-divinylbenzene) resins. *Journal of Applied Polymer Science*, 136(3):1–7, 2019.

[151] Gaoming Jiang Wanli Xu, Pibo Ma and Ailan Wan. Mechanical Properties of Polypropylene Warp-Knitted Hernia Repair Mesh with Different. 2018.

[152] Xingang Wang, Chunmao Han, Xinlei Hu, Huafeng Sun, Chuangang You, Changyou Gao, and Yang Haiyang. Applications of knitted mesh fabrication techniques to scaffolds for tissue engineering and regenerative medicine. *Journal of the Mechanical Behavior of Biomedical Materials*, 4(7):922–932, 2011.

[153] David J. Spencer. Classes of warp knitting machines. *Knitting Technology*, pages 298–312, 2001.

[154] Yimin Qin. *Medical Textile Materials*. 2015.

[155] Rabiatul Manisah Mohamed and Kamal Yusoh. A Review on the Recent Research of Polycaprolactone (PCL). 1134:249–255, 2016.

[156] J E Mark. *Polymer data handbook*. Oxford University Press, 2, illustr edition, 2009.

[157] Drug Adminis. *POLYCAPROLACTONE : SYNTHESIS , PROPERTIES , AND*. 2017.

[158] Elbay Malikmammadov, Tugba Endogan Tanir, Aysel Kiziltay, Vasif Hasirci, and Nesrin Hasirci. *PCL and PCL-based materials in biomedical applications*, volume 29. Taylor & Francis, 2018.

[159] Marianne Labet and Wim Thielemans. Synthesis of polycaprolactone : a review w. pages 3484–3504, 2009.

[160] Barbora East, Martin Plencner, Martin Kralovic, Michala Rampichova, Vera Sovkova, Karolina Vocetkova, Martin Otahal, Zbynek Tonar, Yaroslav Kolinko, Evzen Amler,

and Jiri Hoch. A polypropylene mesh modified with poly-ϵ-caprolactone nanofibers in hernia repair: Large animal experiment. *International Journal of Nanomedicine*, 13:3129–3143, 2018.

[161] Martin Plencner, Eva Prosecká, Michala Rampichová, Barbora East, Matej Buzgo, Lucie Vysloužilová, Jiří Hoch, and Evžen Amler. Significant improvement of biocompatibility of polypropylene mesh for incisional hernia repair by using poly-ϵ-caprolactone nanofibers functionalized with thrombocyte-rich solution. *International Journal of Nanomedicine*, 10(May):2635–2646, 2015.

[162] Signe Gellert Hansen, Mehmet Berat Taskin, Menglin Chen, Lise Wogensen, Jens Vinge Nygaard, and Susanne Maigaard Axelsen. Electrospun nanofiber mesh with fibroblast growth factor and stem cells for pelvic floor repair. *Journal of Biomedical Materials Research - Part B Applied Biomaterials*, 108(1):48–55, 2020.

[163] Helena Knopf-Marques, Martin Pravda, Lucie Wolfova, Vladimir Velebny, Pierre Schaaf, Nihal Engin Vrana, and Philippe Lavalle. Hyaluronic Acid and Its Derivatives in Coating and Delivery Systems: Applications in Tissue Engineering, Regenerative Medicine and Immunomodulation. *Advanced Healthcare Materials*, 5(22):2841–2855, 2016.

[164] Publisher Taylor, Sei K Hahn, Sandra Jelacic, Ronald V Maier, S Patrick, and Allan S Hoffman. Anti-inflammatory drug delivery from hyaluronic acid hydrogels. (April 2013):37–41, 2012.

[165] Hydrogen Peroxide and Copper Ion. Efficient Degradation of High-Molecular-Weight Hyaluronic Acid by a Combination of Ultrasound ,. 2019.

[166] Bryan P Toole. HYALURONAN : FROM EXTRACELLULAR GLUE TO PERICELLULAR CUE. 4(July):528–539, 2004.

[167] Bruna Corradetti, Francesca Taraballi, Jonathan O Martinez, Silvia Minardi, Guillermo Bauza, Michael Evangelopoulos, Sebastian Powell, and Claudia Corbo. Hyaluronic acid coatings as a simple and efficient approach to improve MSC homing toward the site of inflammation. *Scientific Reports*, (July):1–12, 2017.

[168] C Antich, R Sabata, J A Marchal, C U Fuentenueva, and Advanced Therapies Area. ADVANCES OF HYALURONIC ACID IN STEM CELL THERAPY AND TISSUE ENGINEERING , INCLUDING CURRENT CLINICAL TRIALS. 2019.

[169] Jaime M Cyphert, Carol S Trempus, and Stavros Garantziotis. Size Matters : Molecular Weight Specificity of Hyaluronan Effects in Cell Biology. 2015, 2015.

[170] J. F. Gillion, G. Fromont, M. Lepère, N. Letoux, A. Dabrowski, C. Zaranis, and C. Barrat. Laparoscopic ventral hernia repair using a novel intraperitoneal lightweight mesh coated with hyaluronic acid: 1-year follow-up from a case–control study using the Hernia-Club registry. *Hernia*, 20(5):711–722, 2016.

[171] Ladan Espandar, Bruce Bunnell, Guo Yong Wang, Paula Gregory, Christine McBride, and Majid Moshirfar. Adipose-Derived Stem Cells on Hyaluronic Acid–Derived Scaffold: A New Horizon in Bioengineered Cornea. *Archives of Ophthalmology*, 130(2):202–208, feb 2012.

[172] Smitha Mathews, Ramesh Bhonde, Pawan Kumar Gupta, and Satish Totey. A novel tripolymer coating demonstrating the synergistic effect of chitosan, collagen type 1 and hyaluronic acid on osteogenic differentiation of human bone marrow derived mesenchymal stem cells. *Biochemical and Biophysical Research Communications*, 414(1):270–276, 2011.

[173] Yuguo Lei, Shiva Gojgini, Jonathan Lam, and Tatiana Segura. The spreading, migration and proliferation of mouse mesenchymal stem cells cultured inside hyaluronic acid hydrogels. *Biomaterials*, 32(1):39–47, 2011.

[174] Esmat Alemzadeh, Ahmad Oryan, and Ali A. Mohammadi. Hyaluronic acid hydrogel loaded by adipose stem cells enhances wound healing by modulating IL-1β, TGF-β1, and bFGF in burn wound model in rat. *Journal of Biomedical Materials Research - Part B Applied Biomaterials*, 108(2):555–567, 2020.

[175] Saliha Rizvi, Syed T. Raza, Faizal Ahmed, Absar Ahmad, Shania Abbas, and Farzana Mahdi. The role of Vitamin E in human health and some diseases. *Sultan Qaboos University Medical Journal*, 14(2):157–165, 2014.

[176] P. M. Bramley, I. Elmadfa, A. Kafatos, F. J. Kelly, Y. Manios, H. E. Roxborough, W. Schuch, P. J.A. Sheehy, and K. H. Wagner. Vitamin E. *Journal of the Science of Food and Agriculture*, 80(7):913–938, 2000.

[177] Etsuo Niki. Evidence for beneficial effects of vitamin E. *Korean Journal of Internal Medicine*, 30(5):571–579, 2015.

[178] A S Nazrun, M Norazlina, M Norliza, and S Ima Nirwana. The Anti-Inflammatory Role of Vitamin E in Prevention of Osteoporosis. 2012, 2012.

[179] Asli Celebioglu and Tamer Uyar. Antioxidant Vitamin E / Cyclodextrin Inclusion Complex Electrospun Nanofibers : Enhanced Water Solubility , Prolonged Shelf Life , and Photostability of Vitamin E Antioxidant Vitamin E / Cyclodextrin Inclusion Complex Electrospun Nanofibers : Enhanced Wat. (February), 2018.

[180] Gurkan Yetkin, Mehmet Uludag, Bulent Citgez, Sinan Karakoc, Nedim Polat, and Fevziye Kabukcuoglu. Prevention of peritoneal adhesions by intraperitoneal administration of vitamin E and human amniotic membrane. *International Journal of Surgery*, 7(6):561–565, 2009.

[181] Fernando De La Portilla, Ignacio Ynfante, Daniel Bejarano, Jaime Conde, Ana Fernández, José Ma Ortega, and Gonzalo Carranza. Prevention of peritoneal adhesions by intraperitoneal administration of vitamin E: An experimental study in rats. *Diseases of the Colon and Rectum*, 47(12):2157–2161, 2004.

[182] Vimal K Singh, Abhishek Saini, Manisha Kalsan, and Neeraj Kumar. Describing the Stem Cell Potency : The Various Methods of Functional Assessment and In silico Diagnostics. 4(November), 2016.

[183] Daniel Howard, Lee D Buttery, Kevin M Shakesheff, and Scott J Roberts. Tissue engineering : strategies , stem cells and scaffolds. pages 66–72, 2008.

[184] M.D. Andrew M. Altman and M.D. Feras J. Abdul Khalek, M.D. Eckhard U. Alt, M.D., Ph.D. Charles E. Butler. Adipose Tissue–Derived Stem Cells Enhance Bioprosthetic Mesh Repair of Ventral Hernias Andrew. *PRS Journal*, pages 845–854, 2010.

[185] Charles J Dolce, Dimitrios Stefanidis, and Jennifer E Keller. Pushing the envelope in biomaterial research : initial results of prosthetic coating with stem cells in a rat model. pages 2687–2693, 2010.

[186] Rebeca Blázquez, Francisco Miguel Sánchez-margallo, Verónica Álvarez, Alejandra Usón, and Javier G Casado. Surgical meshes coated with mesenchymal stem cells provide an anti-inflammatory environment by a M2 macrophage polarization. 2015.

[187] O. Guillaume, B. Pérez-Köhler, B. Schädl, C. Keibl, N. Saxenhuber, P. Heimel, E. Priglinger, S. Wolbank, H. Redl, A. Petter-Puchner, and R. Fortelny. Stromal vascular fraction cells as biologic coating of mesh for hernia repair. *Hernia*, 2020.

[188] H U I Cheng, Yanling Zhang, B E I Zhang, J I E Cheng, Weiqi Wang, and X I N Tang. Biocompatibility of polypropylene mesh scaffold with adipose-derived stem cells. pages 2922–2926, 2017.

[189] Erik T. Criman, Wendy E. Kurata, Karen W. Matsumoto, Harry T. Aubin, Carmen E. Campbell, and Lisa M. Pierce. Bone marrow-derived mesenchymal stem cells enhance bacterial clearance and preserve bioprosthetic integrity in a model of mesh infection. *Plastic and Reconstructive Surgery - Global Open*, 4(6):1–8, 2016.

[190] Arnab Majumder, Yue Gao, Emanuel E Sadava, James M Anderson, and Yuri W Novitsky. Cell-coating affects tissue integration of synthetic and biologic meshes : comparative analysis of the onlay and underlay mesh positioning in rats. *Surgical Endoscopy*, 2016.

[191] Yue Gao, David M Krpata, Cory N Criss, and Yuri W Novitsky. Effects of mesenchymal stem cell and fibroblast coating on immunogenic potential of prosthetic meshes in vitro. pages 2357–2367, 2014.

[192] Yilin Zhao, Zhigang Zhang, Jinling Wang, Ping Yin, Jianyin Zhou, Maochuan Zhen, Wugeng Cui, Gang Xu, Donghai Yang, and Zhongchen Liu. Abdominal Hernia Repair With a Decellularized Dermal Scaffold Seeded With Autologous Bone Marrow-Derived Mesenchymal Stem Cells. 36(6):247–255, 2012.

[193] Gian Marco Palini, Lucia Morganti, Filippo Paratore, Federico Coccolini, Giacomo Crescentini, Matteo Nardi, and Luigi Veneroni. Challenging abdominal incisional hernia repaired with platelet-rich plasma and bone marrow-derived mesenchymal stromal cells. A case report. *International Journal of Surgery Case Reports*, 37:145–148, 2017.

[194] Xu Zhou, Yifei Zheng, Jinling Wang, and Yaozong Wang. Preparation of a nano- and micro-fibrous decellularized scaffold seeded with autologous mesenchymal stem cells for inguinal hernia repair. pages 1441–1452, 2017.

[195] C I Borbolla-torres, Luis M Palacios-pineda, Nicol A Ulloa-castillo, and Alex El. Composite Polycaprolactone Membranes Reinforced with TiO 2 Nanoparticles. 2019.

[196] Fariba Safaei, Shahla Khalili, Saied Nouri Khorasani, Laleh Ghasemi-Mobarakeh, and Rasoul Esmaeely Neisiany. Porogen Effect of Solvents on Pore Size Distribution of Solvent-Casted Polycaprolactone Thin Films. *Journal of Polymer Science and Engineering*, 1(4):1–5, 2018.

[197] Milad Fadaie, Esmaeil Mirzaei, Bita Geramizadeh, and Zahra Asvar. Incorporation of nanofibrillated chitosan into electrospun PCL nanofibers makes scaffolds with enhanced mechanical and biological properties Milad. *Carbohydrate Polymers*, 2018.

[198] Karina Ángel-sánchez, César I Borbolla-torres, and Luis M Palacios-pineda. Development , Fabrication , and Characterization of Composite Polycaprolactone Membranes Reinforced with TiO 2 Nanoparticles. pages 1–14, 2019.

[199] Jie Chen, Cheng Peng, Jun Nie, John F Kennedy, and Guiping Ma. Lyophilization as a novel approach for preparation of water resistant HA fiber membranes by crosslinked with EDC. *Carbohydrate Polymers*, 102:8–11, 2014.

[200] Arianna Fallacara, Filippo Marchetti, Michele Pozzoli, and Ugo Raffaello Citernesi. Formulation and Characterization of Native and Crosslinked Hyaluronic Acid Microspheres for Dermal Delivery of Sodium Ascorbyl Phosphate : A Comparative Study. pages 1–21, 2018.

[201] Sadanand Pandey and Shivani B Mishra. Graft copolymerization of ethylacrylate onto xanthan gum , using potassium peroxydisulfate as an initiator International Journal of Biological Macromolecules Graft copolymerization of ethylacrylate onto xanthan gum , using potassium peroxydisulfate as an initiator. *International Journal of Biological Macromolecules*, 49(4):527–535, 2019.

[202] E. Fernholz. THE THERMAL DECOMPOSITION OF α-TOCOPHEROL. *Journal of the American Chemical Society*, 59(6):1154–1155, may 2002.

[203] Ohki Kambara, Atsuo Tamura, Takashi Uchino, Kohji Yamamoto, and Keisuke Tominaga. Terahertz time-domain spectroscopy of poly-L-lysine. *Biopolymers*, 93(8):735–739, 2010.

[204] Niharika Lal, Juhi Dubey, Praveen Gaur, Navneet Verma, and Anurag Verma. Chitosan based in situ forming polyelectrolyte complexes: A potential sustained drug delivery polymeric carrier for high dose drugs. *Materials Science & Engineering C*, 2017.

[205] Bruno C Silva, Sabrina Alves, De Oliveira, Bruno Campos, Izabel Cristina Riegelvidotti, Alexandre Urbano, Paula Cristina, De Sousa Faria-tischer, and Cesar Augusto. Production and characterization of bacterial cellulose membranes with hyaluronic acid from chicken comb. *International Journal of Biological Macromolecules*, 97(January):642–653, 2017.

[206] Benarbia Abderrahim, Elidrissi Abderrahman, Aqil Mohamed, Tabaght Fatima, and Tahani Abdesselam. Kinetic Thermal Degradation of Cellulose , Polybutylene Succinate and a Green Composite : Comparative Study. 3(4):95–110, 2015.

[207] National Institute of Standards and Technology. α-Tocopherol acetate, 2018.

[208] Chen Guang-Mei, Zou Tie-Mei, Chen Lei, and Huang Yi-Ping. Crystallization properties of polycaprolactone induced by different hydroxyapatite nano-particles. *Asian Journal of Chemistry*, 22(8):5902–5912, 2010.

[209] Mariana Sato de S. B. Monteiro and Maria Inês Bruno Tavares. The Development and Characterization of Polycaprolactone and Titanium Dioxide Hybrids. *Advances in Nanoparticles*, 07(01):11–27, 2018.

[210] M Ravi, Shenhua Song, Jingwei Wang, Xin Tang, and Zhongyi Zhang. Preparation and characterization of biodegradable poly (ϵ -caprolactone) -based gel polymer electrolyte films.

[211] Sapna Sethi, Saruchi, Balbir Singh Kaith, Mandeep Kaur, Neeraj Sharma, and Vaneet Kumar. Cross-linked xanthan gum–starch hydrogels as promising materials for controlled drug delivery. *Cellulose*, 0, 2020.

[212] H S Abdo, A A Elzatahry, H F Alharbi, and K A Khalil. 2 - Electrical Conductivity Behavior of Biopolymer Composites. In K K Sadasivuni, D Ponnamma, J Kim, J.-J. Cabibihan, and M A AlMaadeed, editors, *Biopolymer Composites in Electronics*, pages 13–25. Elsevier, 2017.

[213] B Saad and U W Suter. Biodegradable Polymeric Materials. In K H Jürgen Buschow, Robert W Cahn, Merton C Flemings, Bernhard Ilschner, Edward J Kramer, Subhash Mahajan, and Patrick Veyssière, editors, *Encyclopedia of Materials: Science and Technology*, pages 551–555. Elsevier, Oxford, 2001.

[214] Alisha Prabhakar, Amy P. Lynch, and Mark Ahearne. Self-Assembled Infrapatellar Fat-Pad Progenitor Cells on a Poly-ϵ-Caprolactone Film For Cartilage Regeneration. *Artificial Organs*, 40(4):376–384, 2016.

[215] Elaine M. Harnett, John Alderman, and Terri Wood. The surface energy of various biomaterials coated with adhesion molecules used in cell culture. *Colloids and Surfaces B: Biointerfaces*, 55(1):90–97, 2007.

[216] Wei Han Lang, Giulia Calloni, and R. Martin Vabulas. Polylysine is a Proteostasis Network-Engaging Structural Determinant. *Journal of Proteome Research*, 17(5):1967–1977, 2018.

[217] Boo Young Shin and Do Hung Han. Viscoelastic properties of PLA/PCL blends compatibilized with different methods. *Korea Australia Rheology Journal*, 29(4):295–302, 2017.

Curriculum Vitae

(Only one page) Master student was born in Monterrey, México, on December 25, 2208. He earned the Systems Engineering degree from the Instituto Tecnológico y de Estudios Superiores de Monterrey, Monterrey Campus in May 2008. He was accepted in the graduate programs in Information Technologies and Electronics in May 2010.

This document was typed in using LaTeX 2_ε[a] by Alejandro Castañeda Sáenz.

[a]The style file `phdThesisFormat.sty` used to set up this thesis was prepared by the Center of Intelligent Systems of the Instituto Tecnológico y de Estudios Superiores de Monterrey, Monterrey Campus